

Rare Kaon and Pion Decays¹

Laurence Littenberg

Brookhaven National Laboratory, Upton, NY 11973

Abstract. Recent results on rare kaon and pion decays are reviewed and prospects for future experiments are discussed.

INTRODUCTION

The study of kaon and pion rare decays has three primary motivations. The first is the search for physics beyond the Standard Model (BSM). Virtually all attempts to redress the theoretical shortcomings of the Standard Model (SM) predict some degree of lepton flavor violation (LFV). Decays such as $K_L \rightarrow \mu^\pm e^\mp$ and $K^+ \rightarrow \pi^+ \mu^+ e^-$ have excellent experimental signatures and can consequently be pursued to remarkable sensitivities. These sensitivities correspond to extremely high energy scales in models where the only suppression is that of the mass of the exchanged field. There are also theories that predict new particles created in kaon or pion decay or the violation of symmetries other than lepton flavor.

The second motivation is the potential of decays that are allowed but that are extremely suppressed in the SM. In several kaon decays, the leading component is a G.I.M.-suppressed[1] one-loop process that is quite sensitive to fundamental SM parameters such as V_{td} . These decays are also potentially very sensitive to BSM physics. One interesting rare pion decay, $\pi^+ \rightarrow \pi^0 e^+ \nu_e$, that is suppressed only by kinematics, can give a very clean measure of V_{ud} , and possibly shed light on an apparent violation of CKM unitarity.

Finally there are long-distance-dominated decays that can test theoretical techniques such as chiral perturbation theory (χ PT) that purport to elucidate the low-energy behavior of QCD. Also, information from some of these decays is required to extract fundamental information from certain of the one-loop processes.

This field is quite active, as indicated by Table 1, that lists the rare decays for which results have been forthcoming in the last couple of years, as well as those that are under analysis. In the face of such riches, one must be quite selective in a short review such as this.

¹ Lectures given at the PSI Summer School on Particle Physics 18-24 Aug 2002

TABLE 1. Rare K decay modes under recent or on-going study.

$K^+ \rightarrow \pi^+ \nu \bar{\nu}$	$K_L \rightarrow \pi^0 \nu \bar{\nu}$	$K_L \rightarrow \pi^0 \mu^+ \mu^-$	$K_L \rightarrow \pi^0 e^+ e^-$
$K^+ \rightarrow \pi^+ \mu^+ \mu^-$	$K^+ \rightarrow \pi^+ e^+ e^-$	$K_L \rightarrow \mu^+ \mu^-$	$K_L \rightarrow e^+ e^-$
$K^+ \rightarrow \pi^+ e^+ e^- \gamma$	$K^+ \rightarrow \pi^+ \pi^0 \nu \bar{\nu}$	$K_L \rightarrow e^\pm e^\mp \mu^\pm \mu^\mp$	$K^+ \rightarrow \pi^+ \pi^0 \gamma$
$K_L \rightarrow \pi^+ \pi^- \gamma$	$K_L \rightarrow \pi^+ \pi^- e^+ e^-$	$K^+ \rightarrow \pi^+ \pi^0 e^+ e^-$	$K^+ \rightarrow \pi^0 \mu^+ \nu \gamma$
$K_L \rightarrow \pi^0 \gamma \gamma$	$K^+ \rightarrow \pi^+ \gamma \gamma$	$K^+ \rightarrow \mu^+ \nu \gamma$	$K^+ \rightarrow e^+ \nu e^+ e^-$
$K^+ \rightarrow \mu^+ \nu e^+ e^-$	$K^+ \rightarrow e^+ \nu \mu^+ \mu^-$	$K_L \rightarrow e^+ e^- \gamma$	$K_L \rightarrow \mu^+ \mu^- \gamma$
$K_L \rightarrow e^+ e^- \gamma \gamma$	$K_L \rightarrow \mu^+ \mu^- \gamma \gamma$	$K_L \rightarrow e^+ e^- e^+ e^-$	$K_L \rightarrow \pi^0 e^+ e^- \gamma$
$K^+ \rightarrow \pi^+ \mu^+ e^-$	$K_L \rightarrow \pi^0 \mu^\pm e^\mp$	$K_L \rightarrow \mu^\pm e^\mp$	$K^+ \rightarrow \pi^- \mu^+ e^+$
$K^+ \rightarrow \pi^- e^+ e^+$	$K^+ \rightarrow \pi^- \mu^+ \mu^+$	$K^+ \rightarrow \pi^+ X^0$	$K_L \rightarrow e^\pm e^\pm \mu^\mp \mu^\mp$
$K^+ \rightarrow \pi^+ \gamma$	$K_L \rightarrow \pi^0 \pi^0 e^+ e^-$		
$\pi^+ \rightarrow \pi^0 e^+ \nu_e$	$\pi^+ \rightarrow e^+ \nu_e$	$\pi^+ \rightarrow e^+ \nu_e \gamma$	$\pi^+ \rightarrow e^+ \nu_e e^+ e^-$
$\pi^+ \rightarrow e^+ \nu_e \nu \bar{\nu}$	$\pi^0 \rightarrow e^+ e^-$	$\pi^0 \rightarrow e^+ e^- e^+ e^-$	$\pi^0 \rightarrow \nu \bar{\nu}$
$\pi^0 \rightarrow \gamma \nu \bar{\nu}$	$\pi^0 \rightarrow 3\gamma$	$\pi^0 \rightarrow \mu e$	

BEYOND THE STANDARD MODEL

The poster children for BSM probes in kaon decay are LFV processes like $K_L \rightarrow \mu e$ and $K^+ \rightarrow \pi^+ \mu^+ e^-$. In principle, these can proceed through neutrino mixing, but the known neutrino mixing parameters limit the rate through this mechanism to a completely negligible level [2]. Thus the observation of LFV in kaon decay would require a new mechanism. Fig.1 shows $K_L \rightarrow \mu e$ mediated by a hypothetical horizontal gauge boson X , compared with the kinematically very similar process $K^+ \rightarrow \mu^+ \nu$ mediated by a W boson.

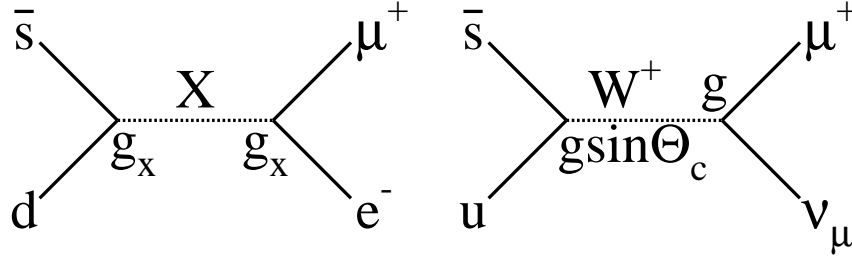


FIGURE 1. Horizontal gauge boson mediating $K_L \rightarrow \mu e$, compared with W mediating $K^+ \rightarrow \mu^+ \nu$.

Using measured values for M_W , the K_L and K^+ decay rates and $B(K^+ \rightarrow \mu^+ \nu)$, and assuming a $V - A$ form for the new interaction, one can show [3]:

$$M_X \approx 220 \text{ TeV}/c^2 \left[\frac{g_X}{g} \right]^{1/4} \left[\frac{10^{-12}}{B(K_L \rightarrow \mu e)} \right]^{1/4} \quad (1)$$

so that truly formidable scales can be probed if $g_X \sim g$. In addition to this generic picture, there are specific models, such as extended technicolor in which LFV at observable levels in kaon decays is quite natural [4].

There were a number of K decay experiments primarily dedicated to lepton flavor violation at the Brookhaven AGS during the 1990's. These advanced the sensitivity to such processes by many orders of magnitude. In addition, several "by-product" results

on LFV and other BSM topics have emerged from the other kaon decay experiments of this period. Rare kaon decay experiments often also yield results on π^0 decays, since these can readily be tagged, *e.g.* via $K^+ \rightarrow \pi^+\pi^0$ or $K_L \rightarrow \pi^+\pi^-\pi^0$. Table 2 summarizes the status of work on BSM probes in kaon and pion decay. The relative reach of these processes is best assessed by comparing the partial rates rather than the branching ratios. From this table it is evident that pion decay is not yet a competitor to kaon decay in probing LFV.

TABLE 2. Current 90% CL limits on K and π decay modes violating the SM. The violation codes are “LF” for lepton flavor, “LN” for lepton number, “G” for generation number, [3], “H” for helicity, “N” requires new particle

Process	Violates	90% CL BR Limit	Γ Limit (sec ⁻¹)	Experiment	Reference
$K_L \rightarrow \mu e$	LF	4.7×10^{-12}	9.1×10^{-5}	AGS-871	[5]
$K^+ \rightarrow \pi^+\mu^+e^-$	LF	2.8×10^{-11}	2.3×10^{-3}	AGS-865	[6]
$K^+ \rightarrow \pi^+\mu^-e^+$	LF, G	5.2×10^{-10}	4.2×10^{-2}	AGS-865	[7]
$K_L \rightarrow \pi^0\mu e$	LF	3.31×10^{-10}	6.4×10^{-3}	KTeV	[8]
$K^+ \rightarrow \pi^-e^+e^+$	LN, G	6.4×10^{-10}	5.2×10^{-2}	AGS-865	[7]
$K^+ \rightarrow \pi^-\mu^+\mu^+$	LN, G	3.0×10^{-9}	2.4×10^{-1}	AGS-865	[7]
$K^+ \rightarrow \pi^-\mu^+e^+$	LF, LN, G	5.0×10^{-10}	4.0×10^{-2}	AGS-865	[7]
$K_L \rightarrow \mu^\pm\mu^\pm e^\mp e^\mp$	LF, LN, G	4.12×10^{-11}	8.0×10^{-4}	KTeV	[9]
$K^+ \rightarrow \pi^+f^0$	N	5.9×10^{-11}	4.8×10^{-3}	AGS-787	[10]
$K^+ \rightarrow \pi^+\gamma$	H	3.6×10^{-7}	2.9×10^1	AGS-787	[11]
$\pi^0 \rightarrow \mu^+e^-$	LF	3.8×10^{-10}	4.5×10^6	AGS-865	[6]
$\pi^0 \rightarrow \mu^-e^+$	LF	3.4×10^{-9}	4.0×10^7	AGS-865	[7]
$\pi^+ \rightarrow \mu^-e^+e^+\nu_e$	LF	1.6×10^{-6}	6.1×10^1	JINR-SPEC	[12]

It is clear from this table that any deviation from the SM must be highly suppressed. The kaon LFV probes in particular have become the victims of their own success. The specific theories they were designed to probe have been killed or at least forced to retreat to the point where meaningful tests in the kaon system would be very difficult. For example, although these decays provide the most stringent limits on strangeness-changing R-violating couplings, the minimal supersymmetric extension of the Standard Model predicts LFV in kaon decay at levels far beyond the current experimental state of the art [13].

Moreover both kaon flux and rejection of background are becoming problematical. Fig.2 shows the signal planes of four of the most sensitive LFV searches. It is clear that background either is already a problem or soon would be if the sensitivity of these searches were increased. Thus new techniques will need to be developed to push such searches significantly further.

Analysis of data already collected is continuing but no new kaon experiments focussed on LFV are being planned. Interest in probing LFV has largely migrated to the muon sector.

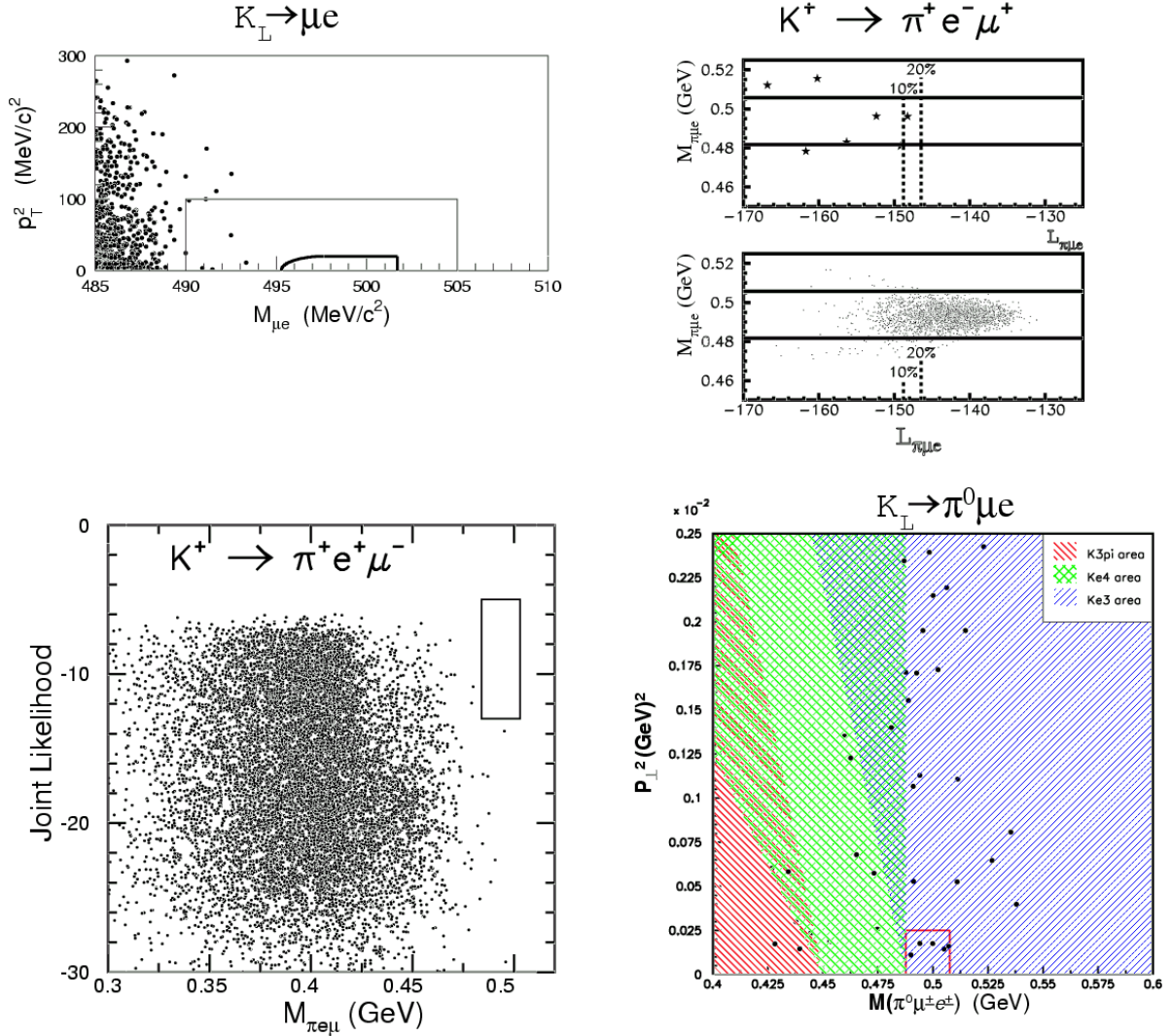


FIGURE 2. Signal planes showing candidates for LFV kaon decays from recent experiments. **Top left:** p_T^2 vs $M_{\mu e}$ from Ref. [5], **Top right:** $M_{\pi\mu e}$ vs Log likelihood from Ref. [6] (lower plot shows signal Monte Carlo), **Bottom left:** Joint likelihood vs $M_{\pi e \mu}$ from Ref. [7], and **Bottom right:** P_\perp^2 vs $M_{\pi\mu e}$ from Ref. [8].

ONE LOOP DECAYS

In the kaon sector the focus of experimental effort has shifted from LFV to “one-loop” decays. These are GIM-suppressed decays in which loops containing weak bosons and heavy quarks dominate or at least contribute measurably to the rate. These processes include $K_L \rightarrow \pi^0 \nu \bar{\nu}$, $K^+ \rightarrow \pi^+ \nu \bar{\nu}$, $K_L \rightarrow \mu^+ \mu^-$, $K_L \rightarrow \pi^0 e^+ e^-$ and $K_L \rightarrow \pi^0 \mu^+ \mu^-$. In some cases the one-loop contributions violate CP. In one, $K_L \rightarrow \pi^0 \nu \bar{\nu}$, this contribution completely dominates the decay[14]. Since the GIM-mechanism enhances the contribution of heavy quarks in the loops, in the SM these decays are sensitive to the product of couplings $V_{ts}^* V_{td}$, often abbreviated as λ_γ . Although one can write the branching ratio

for these decays in terms of the real and imaginary parts of λ_i [15], for comparison with other results such as those from the B system, it is convenient to express them in terms of the Wolfenstein parameters, A , ρ , and η . Fig. 3 relates rare kaon decays to the unitarity triangle. The dashed triangle is the usual one derived from $V_{ub}^*V_{ud} + V_{cb}^*V_{cd} + V_{tb}^*V_{td} = 0$, whereas the solid triangle illustrates the information available from rare kaon decays. Note that the apex, (ρ, η) , can be determined from either triangle, and disagreement between the K and B determinations implies physics beyond the SM. In Fig. 3 the branching ratio closest to each side of the solid triangle can be used to determine the length of that side. The arrows leading outward from those branching ratios point to processes that need to be studied either because they potentially constitute backgrounds, or because knowledge of them is required to relate the innermost branching ratios to the lengths of the triangle sides. $K_L \rightarrow \mu^+\mu^-$, which can determine the bottom of the triangle (ρ), is the process for which the experimental data is the best, but for which the theory is most problematical. $K_L \rightarrow \pi^0\nu\bar{\nu}$, which determines the height of the triangle is theoretically the cleanest, but for this mode experiment is many orders of magnitude short of the SM-predicted level. $K^+ \rightarrow \pi^+\nu\bar{\nu}$, which determines the hypotenuse, is nearly as clean as $K_L \rightarrow \pi^0\nu\bar{\nu}$ and has been observed. Prospects for $K^+ \rightarrow \pi^+\nu\bar{\nu}$ are probably the best of the three since it is clean and it is already clear it can be exploited.

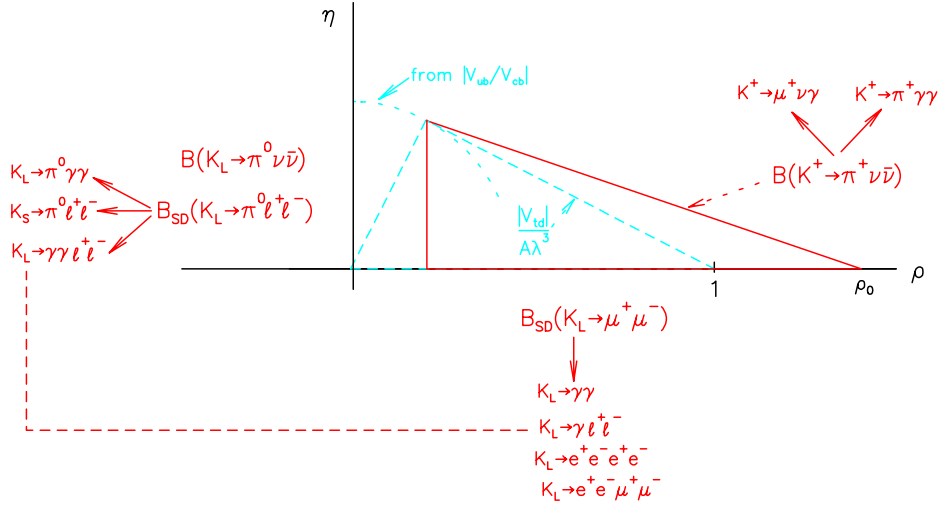


FIGURE 3. K decays and the unitarity plane. The usual unitarity triangle is dashed. The triangle that can be constructed from rare K decays is solid. See text for further details.

$$K_L \rightarrow \mu^+\mu^-$$

The short distance component of this decay, which arises out of the diagrams shown in Fig. 4, can be quite reliably calculated in the SM[16]. The most recent measurement of its branching ratio[17] based on ~ 6200 events gave $B(K_L \rightarrow \mu^+\mu^-) = (7.18 \pm 0.17) \times 10^{-9}$. However $K_L \rightarrow \mu^+\mu^-$ is dominated by long distance effects, the largest of which, the absorptive contribution mediated by $K_L \rightarrow \gamma\gamma$ shown in Fig. 5, accounts for $(7.07 \pm 0.18) \times 10^{-9}$.

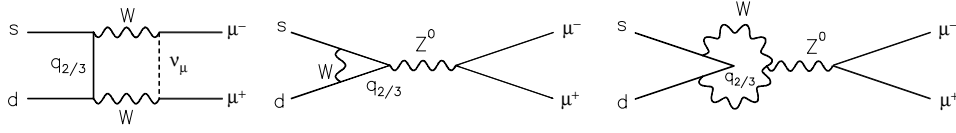


FIGURE 4. Short distance contribution to $K_L \rightarrow \mu^+ \mu^-$ in the SM.

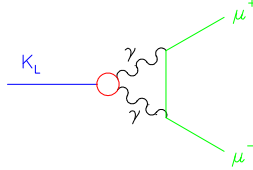


FIGURE 5. Long distance contribution to $K_L \rightarrow \mu^+ \mu^-$.

Subtracting the two, yields a 90% CL upper limit on the total dispersive part of $B(K_L \rightarrow \mu^+ \mu^-)$ of 0.37×10^{-9} . One can do somewhat better than this in the following way. The actual quantity measured in Ref [17] was $B(K_L \rightarrow \mu^+ \mu^-)/B(K_L \rightarrow \pi^+ \pi^-) = (3.48 \pm 0.05) \times 10^{-6}$. It is necessary to subtract from this measured quantity the ratio $B_{\gamma\gamma}^{abs}(K_L \rightarrow \mu^+ \mu^-)B(K_L \rightarrow \pi^+ \pi^-)$. Eqn 2 shows the components of this latter ratio, obtained from Ref. [18] augmented by a new measurement $\Gamma(K_S \rightarrow \pi^+ \pi^-)/\Gamma(K_S \rightarrow \pi^0 \pi^0) = 2.236 \pm 0.003 \pm 0.015$ [19], whose product is $(3.344 \pm 0.053) \times 10^{-6}$.

$$\begin{array}{c}
 \begin{array}{ccc}
 & \text{recently measured} & \\
 & \text{by KLOE} & \\
 & \text{last measured by} & \\
 & \text{NA31 in 1987} & \\
 \text{calculated} & & \frac{B(K_L \rightarrow \pi^0 \pi^0)}{B(K_L \rightarrow \pi^+ \pi^-)} \\
 \downarrow & \downarrow & \downarrow \\
 \frac{B_{\gamma\gamma}^{obs}(K_L \rightarrow \mu\mu)}{B(K_L \rightarrow \pi^+ \pi^-)} = \frac{B_{\gamma\gamma}^{obs}(K_L \rightarrow \mu\mu)}{B(K_L \rightarrow \gamma\gamma)} \frac{B(K_L \rightarrow \gamma\gamma)}{B(K_L \rightarrow \pi^0 \pi^0)} \frac{B(K_S \rightarrow \pi^0 \pi^0)}{B(K_S \rightarrow \pi^+ \pi^-)} (1 - 6Re \frac{\epsilon'}{\epsilon}) \\
 \downarrow & \downarrow & \downarrow \\
 1.195 \cdot 10^{-5} & 0.632 \pm 0.009 & (2.236 \pm 0.015)^{-1} \\
 & & 1 - 6(16.6 \pm 1.6) \cdot 10^{-4} \\
 & & (2)
 \end{array}
 \end{array}$$

The subtraction yields $\frac{B^{disp}(K_L \rightarrow \mu^+ \mu^-)}{B(K_L \rightarrow \pi^+ \pi^-)} = (0.136 \pm 0.073) \times 10^{-6}$ (where B^{disp} refers to the dispersive part of $B(K_L \rightarrow \mu^+ \mu^-)$). $\frac{B^{disp}(K_L \rightarrow \mu^+ \mu^-)}{B(K_L \rightarrow \pi^+ \pi^-)}$ can then be multiplied by $B(K_L \rightarrow \pi^+ \pi^-) = (2.084 \pm 0.032) \times 10^{-3}$ [18] to obtain $B^{disp}(K_L \rightarrow \mu^+ \mu^-) = (0.283 \pm 0.151) \times 10^{-9}$, or $B^{disp}(K_L \rightarrow \mu^+ \mu^-) < 0.47 \times 10^{-9}$ at 90% CL. Note that some of the

components represent 15 year-old measurements. Since $B(K_L \rightarrow \mu^+\mu^-)$ and $B_{\gamma\gamma}^{abs}(K_L \rightarrow \mu^+\mu^-)$ are so close, small shifts in the component values could have relatively large consequences for $B^{disp}(K_L \rightarrow \mu^+\mu^-)$. Several of the components could be remeasured by experiments presently in progress. Now if one inserts the result of even very conservative recent CKM fits into the formula for the short distance part of $B(K_L \rightarrow \mu^+\mu^-)$, one gets poor agreement with the limit of $B^{disp}(K_L \rightarrow \mu^+\mu^-)$ derived above. For example the 95% CL fit of Hocker et al.[20, 21], $\bar{\rho} = 0.07 - 0.37$, gives $B^{SD}(K_L \rightarrow \mu^+\mu^-) = (0.4 - 1.3) \times 10^{-9}$. So why haven't we been hearing about this apparent violation of the SM? There are certainly viable candidates for BSM contributions to this decay [22, 23].

The answer is that unfortunately $K_L \rightarrow \gamma^*\gamma^*$ also gives rise to a dispersive contribution, that is much less tractable than the absorptive part, and which can interfere with the short-distance weak contribution that one is trying to extract. The problem in calculating this contribution is the necessity of including intermediate states with virtual photons of all effective masses. Thus such calculations can only be partially validated by studies of kaon decays containing virtual photons in the final state. The degree to which this validation is possible is controversial with both optimistic [24, 25] and pessimistic [26, 27] conclusions available. Recently there have been talks and publications on $K_L \rightarrow \gamma e^+e^-$ [28] (93,400 events), $K_L \rightarrow \gamma\mu^+\mu^-$ [29] (9327 events), $K_L \rightarrow e^+e^-e^+e^-$ [30] (441 events), and $K_L \rightarrow \mu^+\mu^-e^+e^-$ [9] (133 events) and there exist slightly older high statistics data on $K_L \rightarrow \gamma e^+e^-$ [31] (6864 events). Figure 6-top shows the spectrum of $x = (m_{\mu\mu}/m_K)^2$ from Ref.[29]. The disagreement between the data (filled circles with error bars) and the prediction of pointlike behavior (histogram) clearly indicates the presence of a form factor. A long-standing candidate for this is provided by the BMS model[32] which depends on a single parameter, α_{K^*} .

Fig. 6-bottom shows five determinations of this parameter. The KTeV data are internally consistent, but there's a disagreement with the NA48 result for $K_L \rightarrow e^+e^-\gamma$ [31] Fitting to the more recent DIP parameterization of these decays [24] gives a similar level of agreement. Both these parameterizations predict a connection between the shape of the $\ell^+\ell^-$ spectra and the branching ratios which can be exploited in the cases involving muon pairs. In those cases the parameters have been determined from both the spectra and the branching ratios. These determinations agree at the 1-2 σ level. However the available data is not yet sufficient to clearly favor either parameterization. In addition, it seems clear that a very large increase in the data of processes where both photons are virtual, such as $K_L \rightarrow e^+e^-\mu^+\mu^-$ would be needed to allow a real test of the DIP parameterization [9, 33]. Additional effort, both experimental and theoretical, is required before the quite precise data on $B(K_L \rightarrow \mu^+\mu^-)$ can be fully exploited.

Another possible avenue to understanding long-distance dispersive effects in $K_L \rightarrow \mu^+\mu^-$ may be afforded by the study of $\pi^0 \rightarrow e^+e^-$ where similar effects can come into play[27]. This subject has had somewhat of a checkered history, as indicated in Fig. 7 left, but a 1999 KTeV result in which the π^0 's were tagged in $K_L \rightarrow 3\pi^0$ decays has definitively established the presence of a dispersive term [34]. The clear signal from this experiment is shown in Fig. 7 right. Hopefully theorists will now find this result a useful test-bed.

Finally, one might ask if it is possible to extract short distance information from the decay $K_L \rightarrow e^+e^-$. AGS E871 has seen four events of this mode, establishing a branching

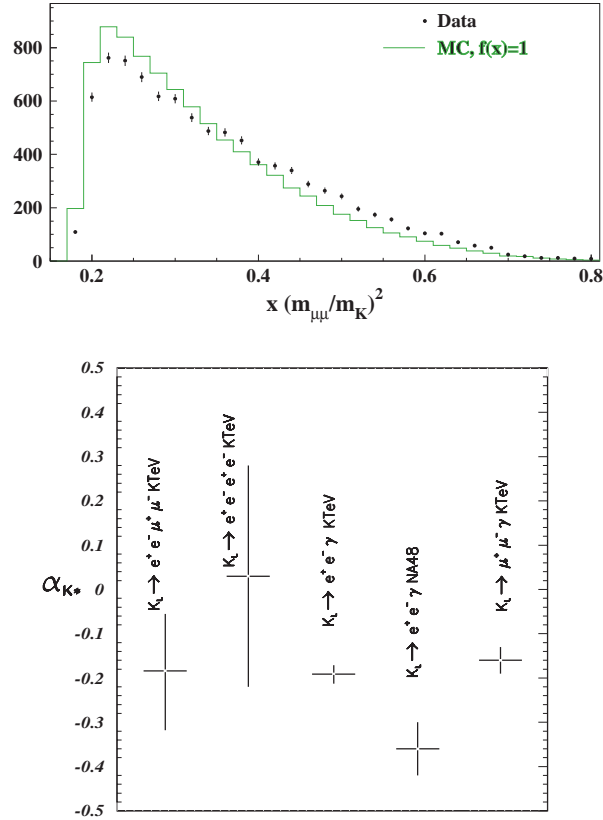


FIGURE 6. **Top:** spectrum of $x = (m_{\mu\mu}/m_K)^2$ in $K_L \rightarrow \mu^+\mu^-\gamma$ from Ref. [29]. **Bottom:** determinations of the BMS parameter α_{K^*} from four K_L decays involving virtual photons.

ratio of $(8.7^{+5.7}_{-4.1}) \times 10^{-12}$ [36]. This is the smallest elementary particle branching ratio yet measured. Unfortunately the SM short distance contribution is helicity suppressed with respect to $K_L \rightarrow \mu^+\mu^-$ by the ratio m_e^2/m_μ^2 while the suppression of long distance contributions is mitigated by logarithmic enhancements, making the extraction of SM short distance information almost impossible. Ironically, the dispersive long-distance contribution can be reliably calculated in this case [26]. The theoretical prediction of the branching ratio agrees well with what is observed, which limits the presence of BSM pseudoscalar couplings in this decay.

$$K^+ \rightarrow \pi^+ \nu \bar{\nu}$$

From the point of view of theory $K^+ \rightarrow \pi^+ \nu \bar{\nu}$ is remarkably clean, suffering none of the long distance complications to which $K_L \rightarrow \mu^+\mu^-$ is subject. The often problematical hadronic matrix element can be calculated to $\sim 2\%$ via an isospin transformation from that of K_{e3} [37]. $K^+ \rightarrow \pi^+ \nu \bar{\nu}$ is very sensitive to V_{td} (it is actually directly sensitive to the quantity $V_{ts}^* V_{td}$). Its amplitude is proportional to the hypotenuse of the solid triangle in Fig. 3. This is equal to the vector sum of the line proportional to $V_{td}/A\lambda^3$ (where

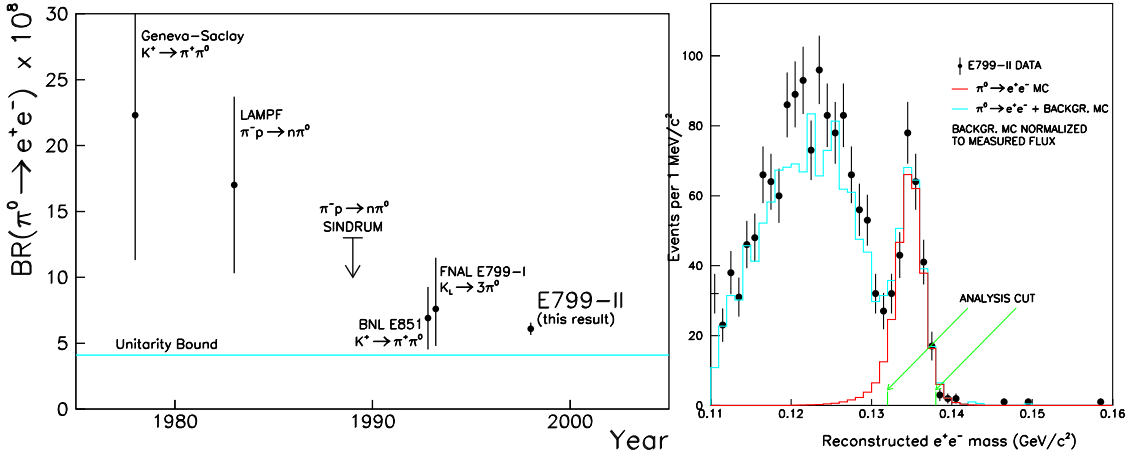


FIGURE 7. **Left:** history of $\pi^0 \rightarrow e^+e^-$ measurements from Ref. [35]. Horizontal line is the absorptive contribution from $\pi^0 \rightarrow \gamma\gamma$. **Right:** Reconstructed m_{ee} distribution for $\pi^0 \rightarrow e^+e^-$ candidates from Ref. [35].

$\lambda \equiv \sin\theta_{Cabibbo}$) and that from $(1, 0)$ to the point marked ρ_0 . The length $\rho_0 - 1$ along the real axis is proportional to the amplitude for the charm contribution to $K^+ \rightarrow \pi^+\nu\bar{\nu}$. The QCD corrections to this amplitude, which are responsible for the largest uncertainty in $B(K^+ \rightarrow \pi^+\nu\bar{\nu})$, have been calculated to NLLA[16]. The residual uncertainty in the charm amplitude is estimated to be $\sim 15\%$ which leads to only a $\sim 6\%$ uncertainty[38] in extracting $|V_{td}|$ from $B(K^+ \rightarrow \pi^+\nu\bar{\nu})$.

Like all previous experiments AGS E787 worked with stopped K^+ . This gives direct access to the K^+ center of mass, and facilitates hermetic vetoing. The detector, shown in Fig. 8 was a cylindrically symmetric solenoid inside a 1 Tesla solenoid [39]. It was situated at the end of a ~ 700 MeV/c electrostatically separated beam that provided an 80% pure supply of $> 10^7$ K^+ per AGS cycle[40]. Beam particles traversed a Cerenkov counter that identified K^+ and π^+ and were tracked through two stations of MWPC's. They were then slowed in a BeO degrader followed by a lead glass photon veto. Approximately one quarter of them survived to exit the lead glass and traverse a hodoscope before entering a scintillating fiber stopping target. A hodoscope surrounding the stopping target was used to trigger on a single charged particle leaving the target after a delay of $\sim 0.12\tau_K$. The particle was subsequently tracked in a low-mass cylindrical drift chamber allowing its momentum to be precisely determined. Additional trigger counters required the particle to exit the chamber radially outward and enter a cylindrical array of scintillators and straw chambers (the Range Stack) in which it was required to stop in order to be considered a $K^+ \rightarrow \pi^+\nu\bar{\nu}$ candidate. The Range Stack scintillation counters were read out by phototubes on both ends which allowed a determination of the position of tracks in the beam direction via differential timing and pulse height. This facility, along with the pattern of pulse heights excited in the counters and the coordinates measured in two layers of straw chambers, determined the range of the stopping particles. The detector design minimized “dead” material so that the kinetic energy could also be well measured. Range/energy/momentum comparison is a powerful discriminator of low energy particle identity. In addition, transient digitizer readout of

the Range Stack photomultipliers allowed the $\pi^+ \rightarrow \mu^+ \rightarrow e^+$ decay chain to be used to identify π^+ 's. The combination of kinematic and life-cycle techniques can distinguish pions from muons with a misidentification rate of $O(10^{-8})$. Surrounding the Range Stack was a cylindrical lead-scintillator veto counter array and adjacent to the ends of the drift chamber were endcap photon veto arrays of CsI-pure modules[41]. There were also a number of auxillary veto counters near the beamline.

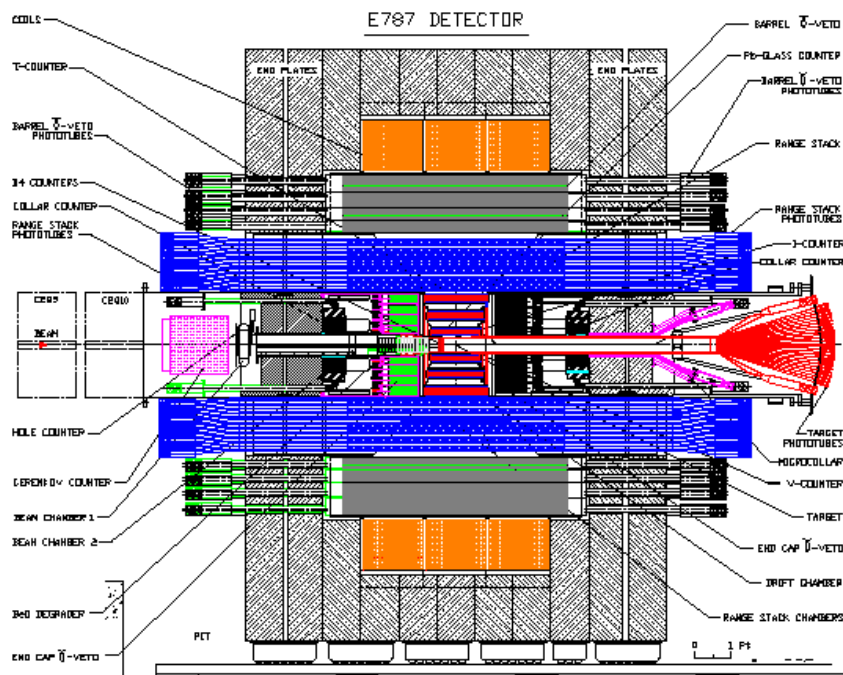


FIGURE 8. E787 detector.

Monte Carlo estimation of backgrounds was in general not reliable since it was necessary to estimate rejection factors as high as 10^{11} for decays occurring in the stopping target. Instead, methods were developed to measure the background from the data itself, using both the primary data stream and data from special triggers taken simultaneously. The principles developed included:

- To eliminate bias – the signal acceptance region is kept hidden while cuts are developed.
- Cuts are developed on 1/3 of the data but residual background levels are measured on the remaining 2/3.
- Bifurcated background calculation. Background sources are identified *a priori*. Two independent cuts with high individual rejection are developed for each background. Each cut is reversed in turn as the other is studied. After optimization, the combined effect of the cuts can then be calculated as a product.
- Cuts are loosened to uncover correlations. If any are found, they are applied before the bifurcation instead of after it, and the background determination process repeated.

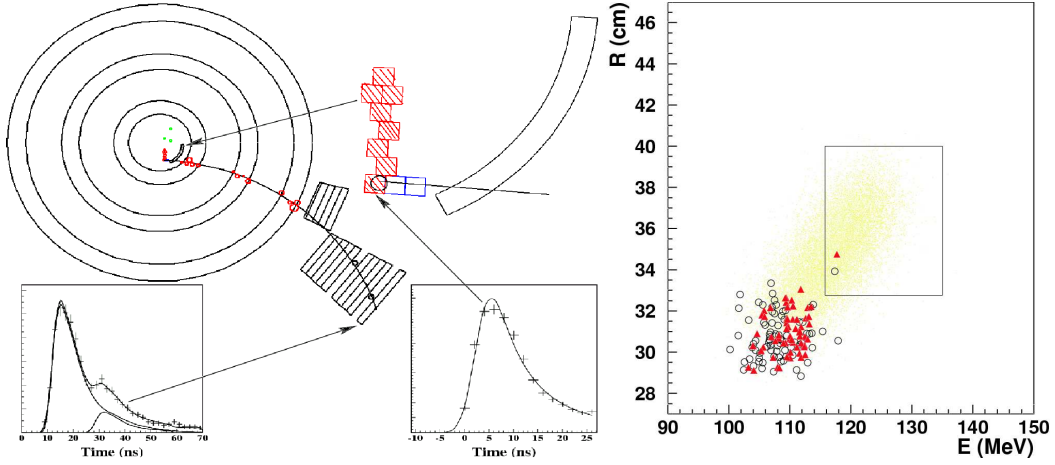


FIGURE 9. **Left:** new $K^+ \rightarrow \pi^+ \nu \bar{\nu}$ event. **Right:** Range vs energy of π^+ in the final sample. The circles are 1998 data and the triangles 1995-7 data. The events around $E = 108$ MeV are $K^+ \rightarrow \pi^+ \pi^0$ background. The simulated distribution of expected signal events is indicated by dots.

- Background calculations are checked by comparison with data near the signal region.

In this way backgrounds can be reliably calculated at the 10^{-3} to 10^{-2} event level.

All factors in the acceptance besides those of solid angle, trigger and momentum interval were determined from data.

Evidence for $K^+ \rightarrow \pi^+ \nu \bar{\nu}$ in the form of a very clean single event candidate was found in data taken in 1995[42]. Subsequent runs in 1996 and 1997 did not produce additional events but in data collected in 1998, a second event was found[10] (see Fig. 9). Combined with previous data [43], this yields a branching ratio $B(K^+ \rightarrow \pi^+ \nu \bar{\nu}) = (1.57^{+1.75}_{-0.82}) \times 10^{-10}$. By comparison, a fit to the CKM phenomenology yields the expectation $(0.72 \pm 0.21) \times 10^{-10}$ [44]. The total background to the two events was measured to be 0.15 of an event *i.e.* $\sim 20\%$ of the signal branching ratio predicted by the SM. Thus E787 has developed methods to reduce the backgrounds to a level sufficient to make a precise measurement of $K^+ \rightarrow \pi^+ \nu \bar{\nu}$, a fact that helped inspire the successor experiment described below.

It is possible to use the E787 result to extract CKM information under various assumptions. One can obtain

$$0.007 < |V_{td}| < 0.030 \quad (68\% \text{ CL}) \quad (3)$$

$$0.005 < |V_{td}| < 0.033 \quad (90\% \text{ CL}) \quad (4)$$

$$|V_{td}| < 0.033 \quad (90\% \text{ CL}) \quad (5)$$

$$-0.022 < \text{Re}V_{td} < 0.030 \quad (68\% \text{ CL}) \quad (6)$$

$$|\text{Im}V_{td}| < 0.028 \quad (90\% \text{ CL}) \quad (7)$$

assuming that $\bar{m}_t(m_t) = 166 \pm 5 \text{ GeV}/c$ and $V_{cb} = 0.041 \pm 0.002$. Alternatively one can extract limits on λ_t that don't depend on V_{cb} :

$$0.29 < |\lambda_t|/10^{-3} < 1.2 \quad (68\% \text{ CL}) \quad (8)$$

$$-0.88 < \text{Re}(\lambda_t)/10^{-3} < 1.2 \quad (68\% \text{ CL}) \quad (9)$$

$$\text{Im}(\lambda_t)/10^{-3} < 1.1 \quad (90\% \text{ CL}) \quad (10)$$

These limits are not competitive with what can be obtained using the full array of available phenomenological information, but they depend on far fewer assumptions. It will be very interesting to compare the large value for $|V_{td}|$ suggested by the E787 result with the value that is eventually extracted from $\bar{B}_s - B_s$ mixing when it is finally observed.

From the first observation published in 1997, E787's results for $B(K^+ \rightarrow \pi^+ \nu \bar{\nu})$ have been rather high with respect to the SM prediction. Although there has never been a statistically significant disagreement with the latter, this has stimulated a number of predictions in BSM theories. Fig 10 shows a selection of such predictions (defined in Table 3) compared with the SM range.

The E787 data also yields an upper limit on the process $K^+ \rightarrow \pi^+ X^0$ where X^0 is a massless weakly interacting particle such as a familon[45]: $B(K^+ \rightarrow \pi^+ X^0) < 5.9 \times 10^{-11}$ at 90% CL. The case of $M_{X^0} > 0$ is discussed below.

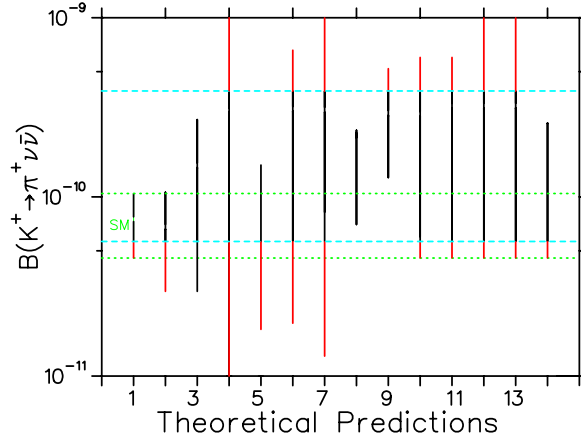


FIGURE 10. Predictions for $B(K^+ \rightarrow \pi^+ \nu \bar{\nu})$. The dashed horizontal lines indicate E787's $\pm 1\sigma$ limits. The dotted horizontal lines indicate the SM range. References are indicated in Table 3

Fig. 11 left shows the π^+ momentum spectrum from $K^+ \rightarrow \pi^+ \nu \bar{\nu}$ in the SM, along with the charged track spectra from other kaon decays.

E787 is sensitive to the filled-in regions of the $K^+ \rightarrow \pi^+ \nu \bar{\nu}$ spectrum in Fig. 11. However all the E787 results mentioned so far come from the region on the right, in which the momentum of the π^+ is greater than than of the π^+ from $K^+ \rightarrow \pi^+ \pi^0$. The region on the left contains more of the signal phase space, but is more subject to background from $K^+ \rightarrow \pi^+ \pi^0$. It is relatively easy for the π^+ to lose energy through nuclear interactions. What is more, there is a problematical correlation between nuclear scattering in the stopping target and the weaker E787 photon veto in the beam region. Fig. 11 right illustrates this problem. A K^+ decays with the π^+ pointing downstream (the π^0 must then be pointing upstream). Normally such a decay would not trigger the

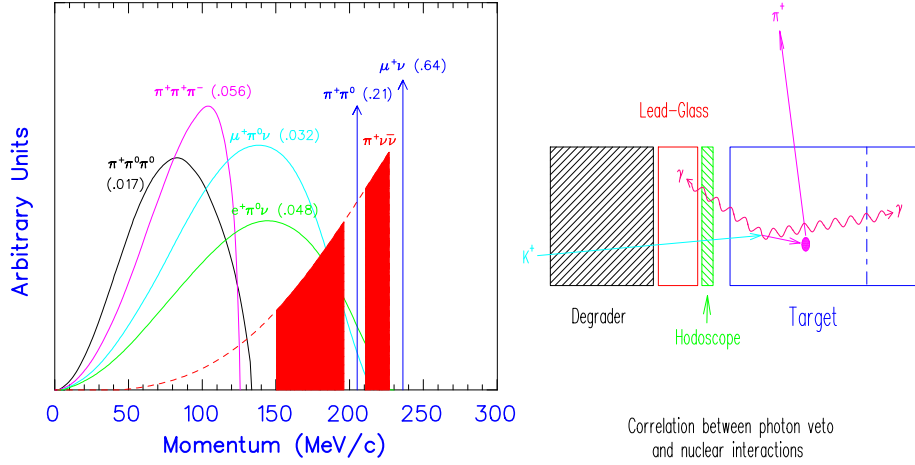


FIGURE 11. Left: Center of mass momentum spectrum of π^+ from $K^+ \rightarrow \pi^+\nu\bar{\nu}$ compared with charged product spectra of the seven most common K^+ decays. Filled areas indicate the portions of the spectrum used in E787 analyses. **Right:** Cartoon of limiting background in the softer region of the $K^+ \rightarrow \pi^+\nu\bar{\nu}$ spectrum. See text for details.

detector, but here the π^+ undergoes a 90° scatter, loses enough energy to get into the accepted momentum range and heads for the drift chamber. At the same time the π^0 decays asymmetrically, with the high energy photon heading upstream, to where the veto is least capable and the low energy photon heading downstream, toward another weak veto region. This sequence of events is unlikely, but 20% of K^+ decay to $\pi^+\pi^0$, and one is trying to study a process that happens one in ten billion times. The fact that the same scatter both down-shifts the π^+ momentum and aims the π^0 at the weak veto region confounds the usual product of rejection factors so effective in the high momentum region. A test analysis using 1996 data was undertaken to determine whether methods could be developed to overcome this background. These leaned heavily on exploiting the

TABLE 3. Predictions for $B(K^+ \rightarrow \pi^+\nu\bar{\nu})$

#	Theory	Ref.
1	Standard Model	[46]
2	MSSM with no new sources of flavor- or CP-violation	[47]
3	Generic SUSY with minimal particle content	[48]
4	Upper limit from Z' limit given by K mass difference	[49]
5	Topcolor	[50]
6	Topcolor-assisted Technicolor Model	[51]
7	Multiscale Walking Technicolor Model	[52]
8	$SU(2)_L \times SU(2)_R$ Higgs	[53]
9	Four generation model	[54]
10	Leptoquarks	[55]
11	R-parity-violating SUSY	[56]
12	Extension of SM to gauge theory of $J = 0$ mesons	[57]
13	Multi Higgs Multiplet Model	[58]
14	Light sgoldstinos	[59]

transient digitized signals from the stopping target target scintillating fibers. At the cost of giving up some acceptance by only using decays later than $0.5 \tau_K$, one could detect evidence of π^+ scattering occluded by kaon signals in the critical target elements. In this way a single event sensitivity of $\sim 10^{-9}$ was achieved with a calculated background of 0.73 events. Fig. 12 left shows the resulting distribution of π^+ kinetic energy and range for surviving candidates. The top left shows the distribution before the final cut on π^+ momentum. The peak at $T_\pi \sim 108$ MeV, $R_\pi \sim 30.5$ cm is due to $K^+ \rightarrow \pi^+\pi^0$ events. After the final cut, one event remains, consistent with the background estimation. This yields $B(K^+ \rightarrow \pi^+\nu\bar{\nu}) < 4.2 \times 10^{-9}$ at 90% CL, consistent with other E787 results. This kinematic region is particularly sensitive to possible BSM effects which produce scalar or tensor pion spectra (rather than the vector spectrum given by the SM). One can combine this region with the high momentum region to get 90% CL upper limits of 4.7×10^{-9} and 2.5×10^{-9} for scalar and tensor interactions, respectively. These measurements are also sensitive to $K^+ \rightarrow \pi^+X^0$ where X^0 is a hypothetical stable weakly interacting particle or system of particles. Fig. 12 right shows 90% CL upper limits on $B(K^+ \rightarrow \pi^+X)$ together with the previous limit from [60]. The dotted line in the figure is the single event sensitivity.

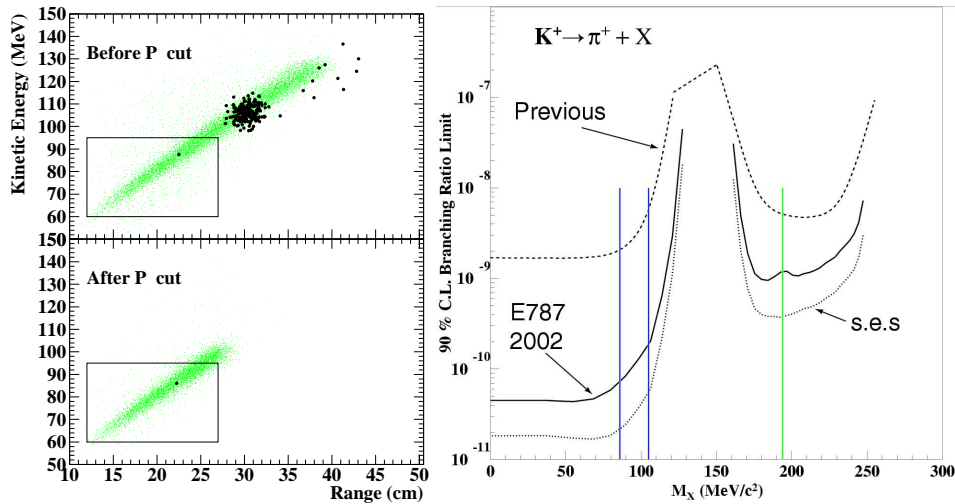


FIGURE 12. Left: Signal plane for $K^+ \rightarrow \pi^+\nu\bar{\nu}$ analysis of soft π^+ region. Right: Limit on $K^+ \rightarrow \pi^+X^0$ vs m_X . Vertical lines indicate location of events. For comparison previous limits are indicated as the single event sensitivity limit of E787.

A new experiment, E949[61], based on an upgrade of the E787 detector has begun operation at the AGS. The detector has been improved in a number of ways with respect to E787: thicker and more complete veto coverage, augmented beam instrumentation, higher capacity DAQ, more efficient trigger counters, upgraded chamber electronics, auxiliary gain monitoring systems, etc. In addition SM sensitivity is anticipated for the kinematic region $140 < p_{\pi^+} < 190$ MeV/c. Several of the upgrades were aimed at exploiting this region, and based on the test analysis discussed above, a signal/background of 1:1 is expected for this part of the spectrum. Using the entire flux of the AGS for 6000 hours, E949 is designed to reach a sensitivity of $\sim 10^{-11}$ /event. The experiment made its first physics run in the Spring of 2002; the detector operated well at fluxes nearly twice as high as those typical of E787.

In June 2001, Fermilab gave Stage 1 approval to an experiment, CKM [62], to extend the study of $K^+ \rightarrow \pi^+ \nu \bar{\nu}$ by yet another order of magnitude in sensitivity. This experiment, unlike all previous ones studying this process, uses an in-flight rather than a stopping K^+ technique. Fig. 13 shows the proposed detector. Protons at 120 GeV/c from the Fermilab Main Injector will be used to produce an RF-separated 22 GeV/c positive beam. The superconducting RF system will produce a 50 MHz positive beam that is $\sim 2/3$ pure K^+ . Incoming kaons will be momentum analyzed in a wire chamber spectrometer and velocity analyzed by a RICH counter with phototube readout. The RICH radiator will be 10m of CF_4 at 0.7 atm. The kaon direction will subsequently be remeasured by a high precision tracker before entering a vacuum decay region in which 17% of the K^+ decay. The upstream section of the decay vacuum will be surrounded by a lead-scintillator sampling calorimeter designed to veto interaction products of the beam kaons in the tracking chambers. Subsequent, wider-bore vacuum vetoes line the remainder of the decay volume. These will be wavelength-shifting fiber readout lead-scintillator sampling calorimeters with 1mm Pb/5mm scintillator granularity and redundant photomultiplier readout. The system is designed to reject photons of energy greater than 1 GeV/c with an inefficiency no greater than 3×10^{-5} . The decay region will be bounded by a straw-chamber-based magnetic spectrometer, also in vacuum. Downstream of the spectrometer will be a second RICH counter, filled with 20m of neon at 1 atm. This counter is designed to tag pions and measure their vector velocity ($\mu - \pi$ separation is 10σ , momentum and angular resolutions are 1% and $200 \mu\text{rad}$ respectively). Downstream of the pion RICH will be an electromagnetic calorimeter covering the full aperture excepting a small hole for the beam. This calorimeter must be highly segmented transversely in order to allow detection of photons that lie close to candidate signal π^+ 's. Following this calorimeter will be a muon veto system in the form of an iron-scintillator hadronic calorimeter. This system is required to reject muons by $10^5 : 1$ for a pion acceptance of 90%. Background photons traversing the beam hole in the forward veto and muon vetoes will be detected in a "hole" veto system, and there must also be an in-beam charged particle veto to catch e^+ and e^- from photon conversions in the pion RICH. The latter will be composed of scintillating fiber planes and will also serve to tag beam particles.

Like E787 and E949, CKM features redundant background rejection techniques. The right hand graph in Fig. 13 shows the expected distribution of candidate events in missing mass squared. The shaded events are the signal, whereas the large peak is due to $K^+ \rightarrow \pi^+ \pi^0$ background.

This experiment is expected to start collecting data in 2007 or 2008.

Fig. 14 shows the history and expectations of progress in studying $K^+ \rightarrow \pi^+ \nu \bar{\nu}$.

$$K_L \rightarrow \pi^0 \nu \bar{\nu}$$

$K_L \rightarrow \pi^0 \nu \bar{\nu}$ is the most attractive target in the kaon system, since it is direct CP-violating to a very good approximation [14, 63] ($B(K_L \rightarrow \pi^0 \nu \bar{\nu}) \propto \eta^2$). Like $K^+ \rightarrow \pi^+ \nu \bar{\nu}$ the hadronic matrix element can be obtained from K_{e3} , but unlike $K^+ \rightarrow \pi^+ \nu \bar{\nu}$, it has no significant contribution from charm. As a result, the intrinsic theoretical uncertainty

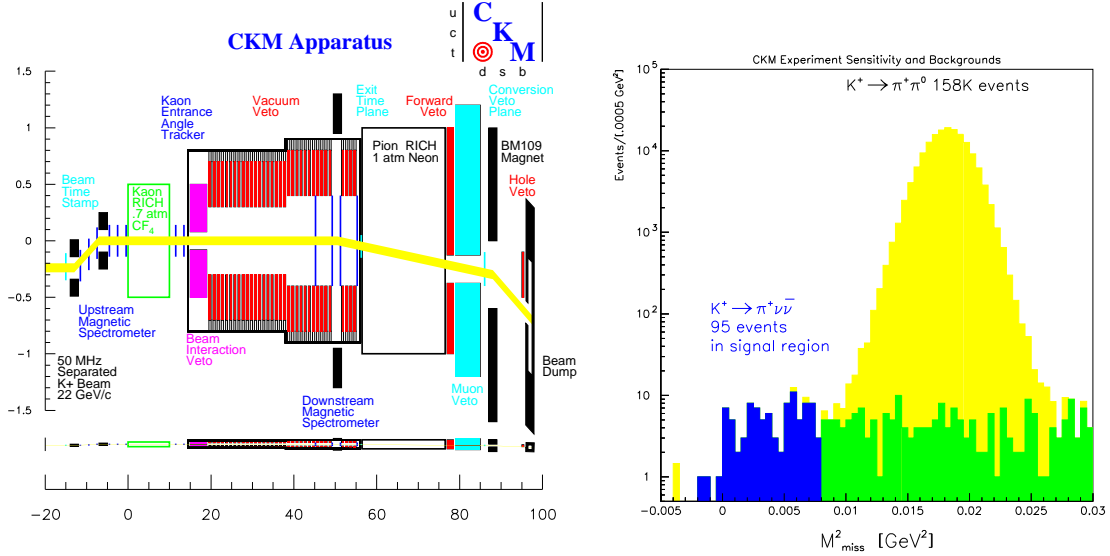


FIGURE 13. Left: apparatus of the CKM experiment at FNAL. Right: expected π signal and background.

connecting $B(K_L \rightarrow \pi^0 \nu \bar{\nu})$ to the fundamental SM parameters is only about 2%. Note also that $B(K_L \rightarrow \pi^0 \nu \bar{\nu})$ is directly proportional to the square of $Im\lambda_t$ and that $Im\lambda_t = -\mathcal{J}/[\lambda(1 - \frac{\lambda^2}{2})]$ where \mathcal{J} is the Jarlskog invariant[64]. Thus a measurement of $B(K_L \rightarrow \pi^0 \nu \bar{\nu})$ determines the area of the unitarity triangles with a precision twice as good as that on $B(K_L \rightarrow \pi^0 \nu \bar{\nu})$ itself.

$B(K_L \rightarrow \pi^0 \nu \bar{\nu})$ can be bounded indirectly by measurements of $B(K^+ \rightarrow \pi^+ \nu \bar{\nu})$ through a nearly model-independent relationship pointed out by Grossman and Nir[65]. The application of this to the new E787 result yields $B(K_L \rightarrow \pi^0 \nu \bar{\nu}) < 1.7 \times 10^{-9}$ at 90% CL. This is far tighter than the current direct experimental limit, 5.9×10^{-7} , obtained by KTeV[66] using $\pi^0 \rightarrow \gamma e^+ e^-$ decay. To actually measure $B(K_L \rightarrow \pi^0 \nu \bar{\nu})$ at the SM level ($\sim 3 \times 10^{-11}$), one will need to improve on this by some five orders of magnitude. Fig. 15 shows the p_T spectrum of events from that experiment along with the calculated backgrounds.

The calculated background was 0.04 events. This would give ~ 800 background events/SM signal event if just scaled up. Clearly the background rejection power of the experiment would need to be improved. This might be possible, but the leading problem of this technique is simply the factor ~ 80 loss of acceptance incurred by confining oneself to Dalitz decays of the π^0 . To get anywhere near the SM level, one will have to use the $\pi^0 \rightarrow \gamma\gamma$ branch and this is in fact the method of all current and planned attempts to detect $K_L \rightarrow \pi^0 \nu \bar{\nu}$.

The KEK E391a experiment[67] proposes to achieve a sensitivity of $\sim 3 \times 10^{-10}$ /event which would better the indirect limit by a factor five, but would not fully bridge the gap between this limit and the SM level. However, it will be sensitive to large BSM contributions to this decay and will serve as a test for a future

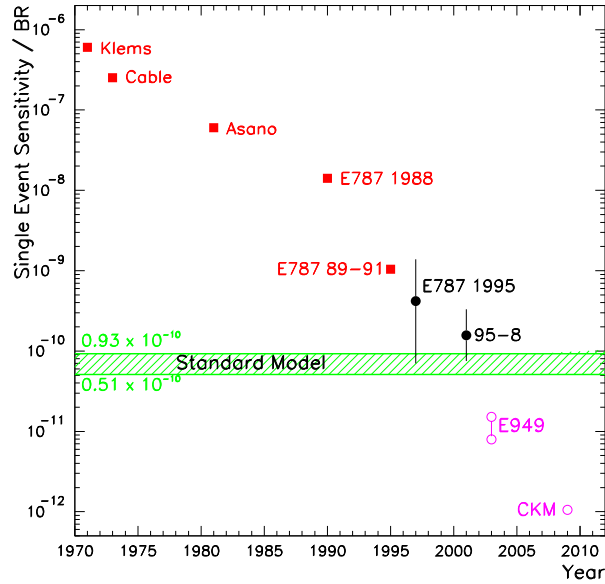


FIGURE 14. History and prospects for the study of $K^+ \rightarrow \pi^+ \nu \bar{\nu}$. Points without error bars are single event sensitivities, those with error bars are measured branching ratio.

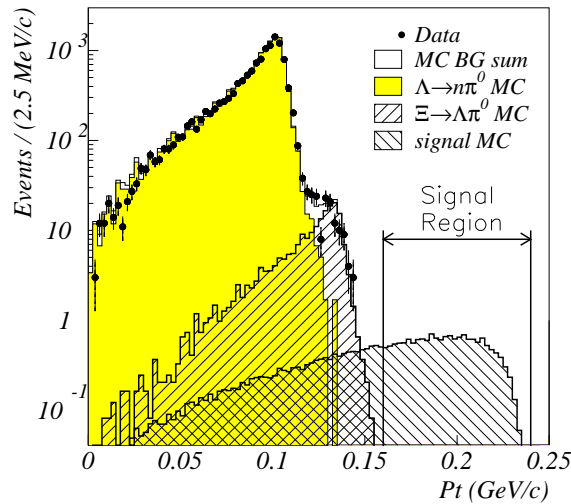


FIGURE 15. P_t spectrum of $K_L \rightarrow \pi^0 \nu \bar{\nu}$ candidates from Ref. [66]

much more sensitive experiment to be performed at the Japanese Hadron Facility. E391a features a carefully designed “pencil” beam with average momentum ~ 3.5 GeV/c. Fig. 16 shows a layout of the detector.

The photon veto system consists of two cylinders. The inner, more upstream barrel is intended to suppress beam halo and reduce confusion from upstream K_L decays. Roughly 4% of the K_L 's decay in the 2.4m fiducial region between the end of the inner

E391a Detector

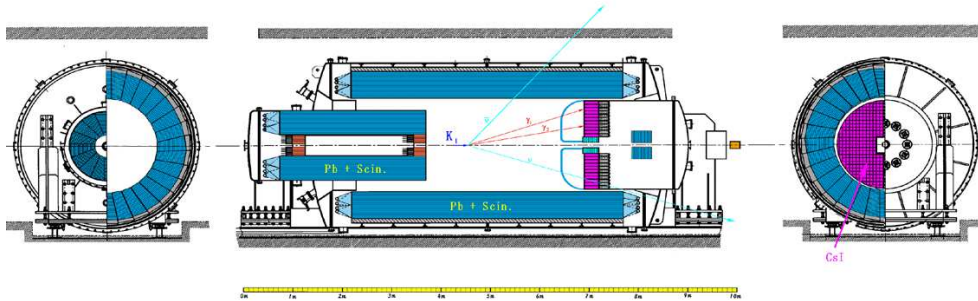


FIGURE 16. KEK E391a detector for $K_L \rightarrow \pi^0 \nu \bar{\nu}$

cylinder and the charged particle veto in front of the photon detector. Signal photons are detected in a multi-element CsI-pure crystal calorimeter. The entire apparatus will operate in vacuum. An advantage of this configuration is rather high acceptance. A particular challenge of this approach is to achieve extremely low photon veto inefficiency. Beam-line construction and tuning started in March 2000 and physics running is expected to begin in Fall, 2003.

The KOPIO experiment[68] at BNL (E926) takes a completely different approach, exploiting the intensity and flexibility of the AGS to make a high-flux, low-energy, microbunched K_L beam. The principles of the experiment are illustrated in Fig. 17.

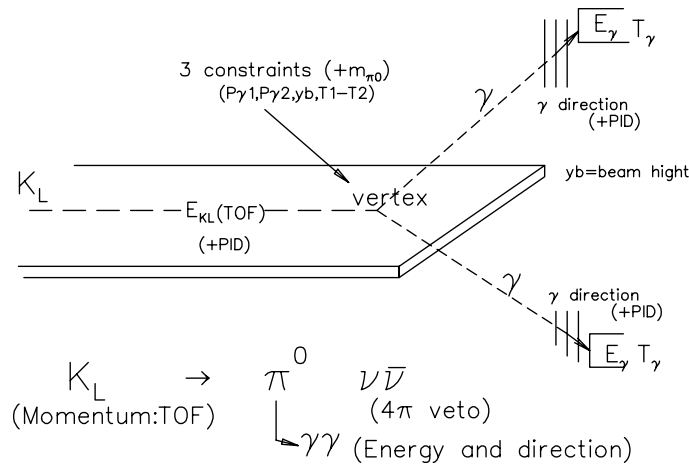


FIGURE 17. Principles of KOPIO $K_L \rightarrow \pi^0 \nu \bar{\nu}$ experiment

The AGS proton beam will be microbunched at 25 MHz by imposing upon it a train of empty RF buckets as it is extracted from the machine[69]. The neutral beam will be extracted at $\sim 45^\circ$ to soften the K_L spectrum sufficiently to permit time-of-flight determination of the K_L velocity. The large production angle also softens the neutron

spectrum so that they (and the K_L) are by and large below threshold for the hadro-production of π^0 's. The beam region will be evacuated to 10^{-7} Torr to further minimize such production. With a 10m beam channel and this low energy beam, the contribution of hyperons to the background will be negligible. The profile of the beam is ribbon-like to facilitate collimation of the large aperture and to provide an extra constraint for reconstruction of the decay vertex. All possible quantities are measured: in addition to the K_L momentum, the photon angles as well as energies and times. In this way, powerful kinematic rejection of background is made possible.

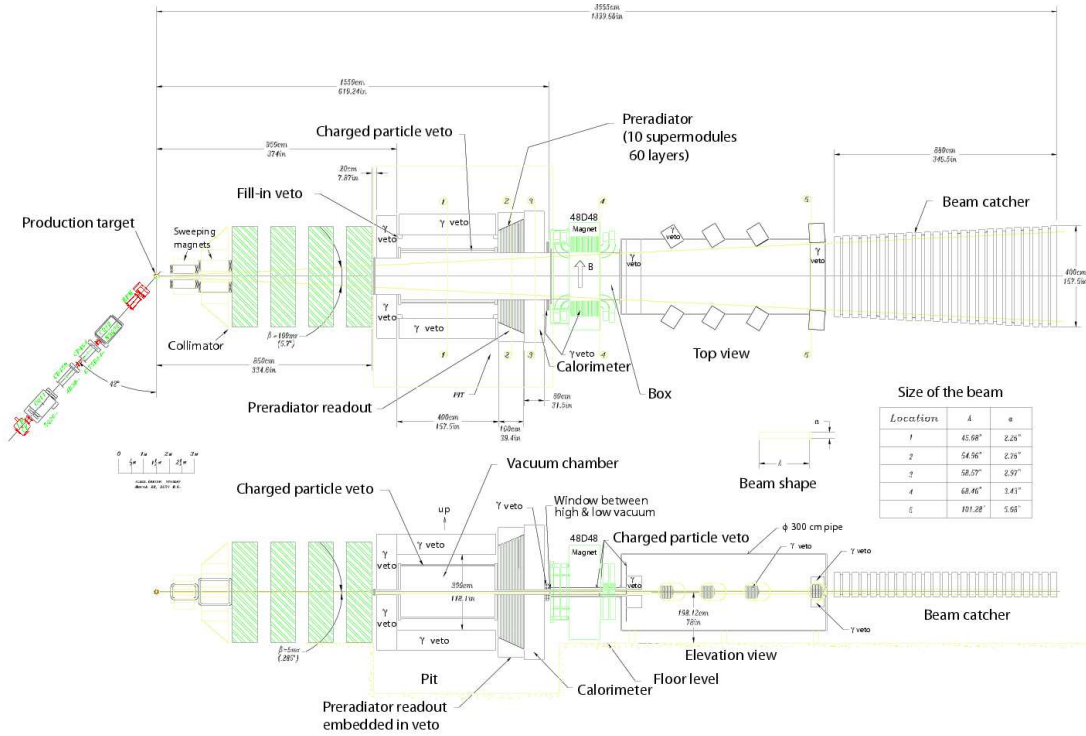


FIGURE 18. Layout of the KOPIO detector.

The layout of the experiment is shown in Fig. 18. K_L decays from a ~ 3 m fiducial region will be accepted. Signal photons impinge on a $2 X_0$ thick preradiator capable of measuring their direction to ~ 30 mrad. An alternating drift chamber/scintillator plane structure will also allow good measurement of the energy deposited in the preradiator. A high-precision shashlyk calorimeter downstream of the preradiator will complete the energy measurement. The photon directional information will allow the decay vertex position to be determined. This can be required to lie within the beam envelope, eliminating many potentially dangerous sources of background. Combined with the target position and time of flight information, the vertex information provides a measurement of the K_L 3-momentum so that kinematic constraints as well as photon vetoing are available to suppress backgrounds. The leading expected background is $K_L \rightarrow \pi^0 \pi^0$, which is initially some eight orders of magnitude larger than the predicted signal. However since π^0 's from this background have a unique energy in the K_L center of mass, a very effective kinematic cut can be applied. This reduces the burden on the photon veto system surrounding the decay region to the point where the hermetic veto techniques proven

in E787 are sufficient. In fact most of the techniques necessary for KOPIO have been proven in previous experiments or in prototype tests. Fig. 19 shows results on two of the more critical aspects of the experiment.

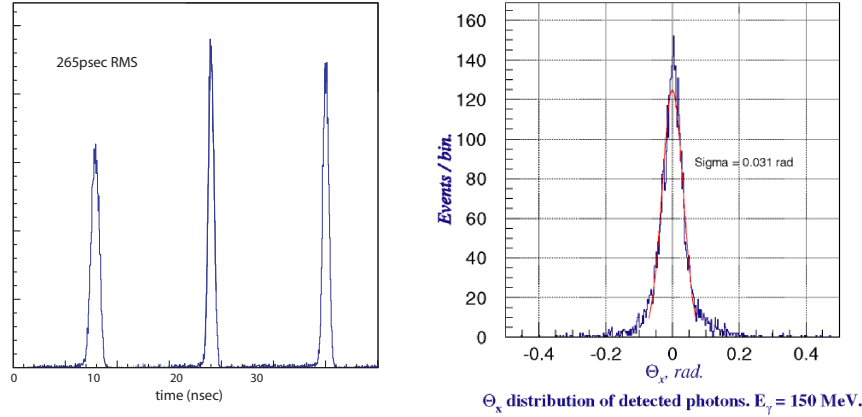


FIGURE 19. Tests of KOPIO components. **Left:** demonstration of microbunching of the AGS proton beam. **Right:** angular resolution of prototype preradiator in a tagged photon beam.

On the left of the figure is the result of a recent test of beam microbunching, showing an rms of 265 psec. This is sufficient for KOPIO's purposes, although it still needs to be demonstrated at a 25 MHz repetition rate. On the right is a plot of photon angular resolution obtained with a 6-plane prototype of the preradiator. A tagged beam at the National Synchrotron Light Source (NSLS) provided the photons. A resolution of 30mrad is observed for 150 MeV photons, in line with GEANT simulation. This resolution is sufficient for KOPIO.

The electromagnetic calorimeter following the preradiator will be a $5.2\text{m} \times 5.2\text{m}$ array of high resolution shashlyk modules. The required resolution of $3\text{-}3.5\%/\sqrt{E}$ has been demonstrated in prototypes tested in the NSLS tagged photon beam.

The upstream and barrel vetoes will be 18 r.l. thick lead-scintillator shower counters read out via wavelength-shifting fibers. The demands on the performance of these counters are comparable to that demonstrated in the E787 barrel veto which has similar structure. Small prototypes have shown good characteristics and full scale prototypes are currently in production. It will also be necessary to veto within the beam, which is very challenging but is facilitated by the low average energy of the beam neutrons. This will be accomplished by a series of lead-aerogel shower counters (the "catcher" veto). For the most part charged particles created by the neutrons are below the Cerenkov threshold of the aerogel and are so invisible to these counters.

Another very important element is charged particle vetoing needed to eliminate backgrounds such as $K_L \rightarrow \pi^0 \pi^+ \pi^-$. A very high performance system will be mounted in the decay region vacuum and at the margins of the downstream beam pipe. Behind the calorimeter will be a dipole magnet with field oriented to sweep charged particles traveling in the beam direction upwards or downwards into veto counters outside the beam profile.

KOPIO aims to collect about 50 $K_L \rightarrow \pi^0 \nu \bar{\nu}$ events with a signal to background ratio of 2:1. This will permit η to be determined to $\sim 10\%$, given expected progress in measuring m_t and V_{cb} . KOPIO will run during the ~ 20 hours/day the AGS is not

needed for injection into RHIC. The experiment is presently in an R&D phase.

$$K_L \rightarrow \pi^0 \ell^+ \ell^-$$

The $K_L \rightarrow \pi^0 \ell^+ \ell^-$ are reactions initially thought to be more tractable experimentally than $K_L \rightarrow \pi^0 \nu \bar{\nu}$. Like $K_L \rightarrow \pi^0 \nu \bar{\nu}$, in the SM they are sensitive to $Im\lambda_t$, but in general they have different sensitivity to BSM effects [48]. Although their signatures are intrinsically superior to that of $K_L \rightarrow \pi^0 \nu \bar{\nu}$, they are subject to a serious background that has no analogue in the neutral lepton case: $K_L \rightarrow \gamma \gamma \ell^+ \ell^-$. This process, a radiative correction to $K_L \rightarrow \gamma \ell^+ \ell^-$, occurs roughly 10^5 times more frequently than $K_L \rightarrow \pi^0 \ell^+ \ell^-$. Kinematic cuts are quite effective, but it is very difficult to improve the signal:background beyond about 1 : 5 [70]. Both varieties of $K_L \rightarrow \gamma \gamma \ell^+ \ell^-$ have been observed, $B(K_L \rightarrow \gamma \gamma e^+ e^-)_{k_\gamma > 5 MeV} = (5.84 \pm 0.15_{stat} \pm 0.32_{syst}) \times 10^{-7}$ [71] and $B(K_L \rightarrow \gamma \mu^+ \mu^-)_{m_{\gamma\gamma} > 1 MeV/c^2} = (10.4^{+7.5}_{-5.9_{stat}} \pm 0.7_{syst}) \times 10^{-9}$ [72]; both agree reasonably well with theoretical prediction. By comparison, the branching ratio arising from SM short distance interactions, $B^{direct}(K_L \rightarrow \pi^0 e^+ e^-)$, is predicted to be [46] $(4.3 \pm 2.1) \times 10^{-12}$ and $B^{direct}(K_L \rightarrow \pi^0 \mu^+ \mu^-)$ about five times smaller.

In addition to this background, there are two other issues that make the extraction of short-distance information from $K_L \rightarrow \pi^0 \ell^+ \ell^-$ rather challenging. First, there is an indirect CP-violating amplitude from the K_1 component of K_L that is proportional to $\epsilon A(K_S \rightarrow \pi^0 e^+ e^-)$. It is of the same order of magnitude as the direct CP-violating amplitude and interferes with it, yielding [73]:

$$B(K_L \rightarrow \pi^0 ee)_{CPV} \approx \left[15.3a_S^2 - 6.8a_S \frac{Im\lambda_t}{10^{-4}} + 2.8 \left(\frac{Im\lambda_t}{10^{-4}} \right)^2 \right] \times 10^{-12} \quad (11)$$

where

$$B(K_S \rightarrow \pi^0 ee) \approx 5.2a_S^2 \times 10^{-9} \quad (12)$$

One can get a very rough estimate of a_S from the related process $K^+ \rightarrow \pi^+ e^+ e^-$, on which there is now rather good data. The corresponding parameter is measured in that decay to be $a_+ = -0.587 \pm 0.010$ [74]. However the dangers of extrapolating from $K^+ \rightarrow \pi^+ e^+ e^-$ to $K_S \rightarrow \pi^0 e^+ e^-$ have been pointed out in Ref. [75]. Thus the size of the indirect CP-violating contribution will be predictable if and when $B(K_S \rightarrow \pi^0 e^+ e^-)$ is measured, hopefully by the upcoming NA48/1 experiment [76]. At the moment our information is limited to $|a_S| < 5.2$ from the NA48 result $B(K_S \rightarrow \pi^0 ee) < 1.4 \times 10^{-7}$ at 90% CL [77].

Another contribution of similar order, mediated by $K_L \rightarrow \pi^0 \gamma \gamma$, is *CP-conserving*. In principle this contribution can be predicted from measurements of the branching ratio and kinematic distributions of $K_L \rightarrow \pi^0 \gamma \gamma$, and thousands of these events have been observed. The matrix element for this decay is given by [78]:

$$\begin{aligned} \mathcal{M}(K_L \rightarrow \pi^0 \gamma \gamma) &= \frac{G_8 \alpha}{4\pi} \epsilon_\mu(k_1) \epsilon_\nu(k_2) [A(k_2^\mu k_1^\nu - k_1 \cdot k_2 g^{\mu\nu}) + \\ &B \frac{2}{m_K^2} (p_k \cdot k_1 k_2^\mu p_K^\nu + p_K \cdot k_2 k_1^\mu p_K^\nu - k_1 \cdot k_2 p_K^\mu p_K^\nu - g^{\mu\nu} p_K \cdot k_1 p_K \cdot k_2)] \end{aligned} \quad (13)$$

where k_1 and k_2 refer to the photons. A and B refer to the $J_\gamma = 0$ and $J_\gamma = 2$ amplitudes respectively, and G_8 is the octet coupling constant in χ PT. Eqn. 13 leads to

$$\frac{\partial^2 \Gamma(K_L \rightarrow \pi^0 \gamma \gamma)}{\partial y \partial z} = \frac{m_K}{2^9 \pi^3} \left[z^2 |A + B|^2 + \left(y^2 - \frac{1}{4} \lambda(1, r_\pi^2, z) \right)^2 |B|^2 \right] \quad (14)$$

where $z \equiv (k_1 + k_2)^2 / m_K^2$, $y \equiv p_K \cdot (k_1 - k_2) / m_K^2$, $r_\pi \equiv m_\pi / m_K$ and $\lambda(a, b, c) \equiv a^2 + b^2 + c^2 - 2(ab + ac + bc)$. Since the effect of A on $K_L \rightarrow \pi^0 e^+ e^-$ is greatly suppressed by helicity conservation and $B = 0$ at leading order in χ PT, it was initially thought that the CP-conserving contribution to $K_L \rightarrow \pi^0 e^+ e^-$ would be very small². However the possibility of a substantial vector meson dominance (VDM) contribution to B was pointed out by Sehgal [79]. Such a contribution can arise at $O(p^6)$ in χ PT. Indeed, early measurements of $B(K_L \rightarrow \pi^0 \gamma \gamma)$ [80, 81] showed that although the simple $O(p^4)$ calculation was in reasonable agreement with the $m_{\gamma\gamma}$ spectrum, it underestimated the decay rate by a factor ~ 3 . There has since been a good deal of theoretical work devoted to remediating this [82, 83, 84, 85, 86]. Although a full $O(p^6)$ calculation is not possible at present, in this work the $O(p^4)$ calculation was improved by ‘‘unitarity corrections’’ and the addition of a VDM contribution characterized by a single parameter a_V . This produced satisfactory agreement with the observed branching ratio, at least until the recent, more precise measurements. A similar approach [87] was successful in predicting the characteristics of the closely related decay $K^+ \rightarrow \pi^+ \gamma \gamma$ that was measured by AGS E787 [88]. The recent data on $K_L \rightarrow \pi^0 \gamma \gamma$ is summarized in Table 4 and the $m_{\gamma\gamma}$ spectra are shown in Fig. 20. Unfortunately the two newest results, from KTeV [89] and from NA48 [90] disagree by nearly 3σ in branching ratio. Their spectra also differ rather significantly, leading to differing extracted values of a_V and thus to disagreement in their predictions for $B^{CP-cons}(K_L \rightarrow \pi^0 e^+ e^-)$, as seen in Table 5. This is inimical to the prospects of measuring $B^{direct}(K_L \rightarrow \pi^0 e^+ e^-)$.

TABLE 4. Recent results on $K_L \rightarrow \pi^0 \gamma \gamma$.

Exp/Ref	$B(K_L \rightarrow \pi^0 \gamma \gamma) \cdot 10^6$	a_V
KTeV [89]	$1.68 \pm 0.07_{stat} \pm 0.08_{syst}$	$-0.72 \pm 0.05 \pm 0.06$
NA48 [77]	$1.36 \pm 0.03_{stat} \pm 0.03_{syst} \pm 0.03_{norm}$	$-0.46 \pm 0.03 \pm 0.03 \pm 0.02_{theor}$

Moreover the use of this formalism to predict $B^{CP-cons}(K_L \rightarrow \pi^0 e^+ e^-)$ from $K_L \rightarrow \pi^0 \gamma \gamma$ has recently been reexamined by Gabbiani and Valencia [92]. They point out that the use of a single parameter a_V artificially correlates the A and B amplitudes. They show that a three parameter expression inspired by $O(p^6)$ χ PT fits the KTeV data quite as well as the conventional one based on a_V and gives a significantly different prediction for $B^{CP-cons}(K_L \rightarrow \pi^0 e^+ e^-)$ as seen in Table 5. In a subsequent paper [93], they find they can make a good simultaneous fit to the NA48 decay rate and spectrum using the same technique and point out that this is not possible using just a_V . The predictions of their three parameter fits for $B^{CP-cons}(K_L \rightarrow \pi^0 e^+ e^-)$ also differ markedly between the two experiments as shown in Table 5.

² There is very little helicity suppression for $K_L \rightarrow \pi^0 \mu^+ \mu^-$ so that the CP-conserving branching ratio is relatively larger.

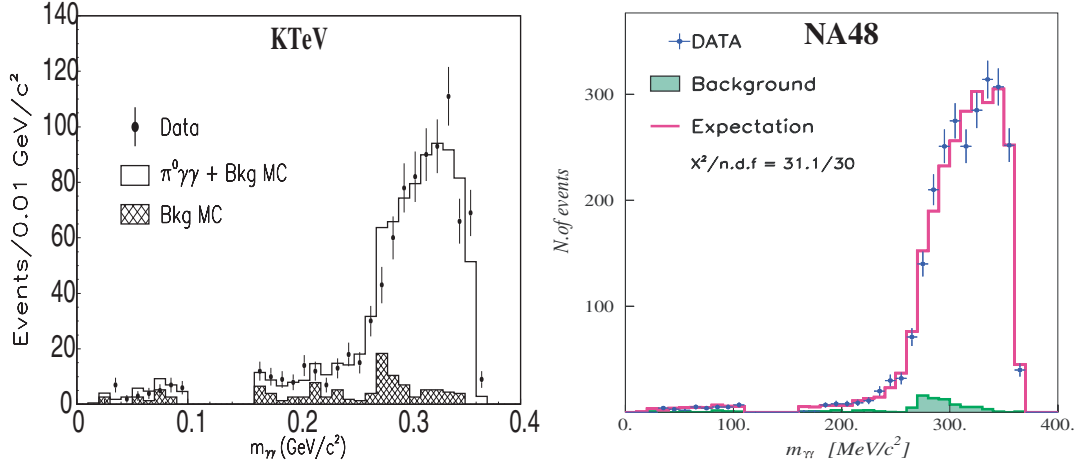


FIGURE 20. $m_{\gamma\gamma}$ spectrum of $K_L \rightarrow \pi^0 \gamma\gamma$ candidates from (left) KTeV [89] and (right) NA48 [90]. The striking threshold at $m_{\gamma\gamma} \approx 2m_\pi$ is due to the amplitude $A(y, z)$ in χ PT (or in pion loop models [91]).

Finally there are significant uncertainties in the extraction of the dispersive contribution to $B^{CP-cons}(K_L \rightarrow \pi^0 e^+ e^-)$ [94, 95], which is similar in size to the absorptive contribution and so not at all negligible.

TABLE 5. Predictions for $B^{CP-cons}(K_L \rightarrow \pi^0 e^+ e^-)$.

Exp.	a_V fit from experimental paper	a_V fit by Gabbiani & Valencia	3 parameter fit by Gabbiani & Valencia
KTeV	$(1.0 - 2.0) \cdot 10^{-12}$	$4.8 \cdot 10^{-12}$	$7.3 \cdot 10^{-12}$
NA48	$(0.47^{+0.22}_{-0.18}) \cdot 10^{-12}$	$(1.38^{+0.09}_{-0.21}) \cdot 10^{-12}$	$(0.46^{+0.22}_{-0.17}) \cdot 10^{-12}$

Thus both the theoretical and experimental situations are quite unsettled at the moment. Depending on which $K_L \rightarrow \pi^0 \gamma\gamma$ data one uses and how one uses it, values from 0.25×10^{-12} to 7.3×10^{-12} are predicted for $B^{CP-cons}(K_L \rightarrow \pi^0 e^+ e^-)$.

The current experimental status of $K_L \rightarrow \pi^0 \ell^+ \ell^-$ is summarized in Table 6 and Fig.21. A factor ~ 2.5 more data is expected from the KTeV 1999 run, but as can be seen from the table and figure, background is already starting to be observed at a sensitivity roughly 100 times short of the expected signal level.

TABLE 6. Results on $K_L \rightarrow \pi^0 \ell^+ \ell^-$.

Mode	90% CL upper limit	Est. bkgnd.	Obs. evts.	Ref.
$K_L \rightarrow \pi^0 e^+ e^-$	5.1×10^{-10}	1.06 ± 0.41	2	[96]
$K_L \rightarrow \pi^0 \mu^+ \mu^-$	3.8×10^{-10}	0.87 ± 0.15	2	[97]

One can get a feeling for the implications of the current data by calculating what it would take to get a 20% measurement of $B^{direct}(K_L \rightarrow \pi^0 e^+ e^-)$ at the SM-predicted level, *i.e.* with precision comparable to what is being discussed for $K_L \rightarrow \pi^0 \nu \bar{\nu}$. The most straightforward case is that where the state-mixing and CP-conserving components turn out to be negligible. One then extrapolates the $K_L \rightarrow \gamma\gamma e^+ e^-$ background in the current experiment, 0.91 ± 0.26 [96], assuming that it gets statistically better determined $\propto 1/\text{sensitivity}$. One finds that without improvements in the background discrimination

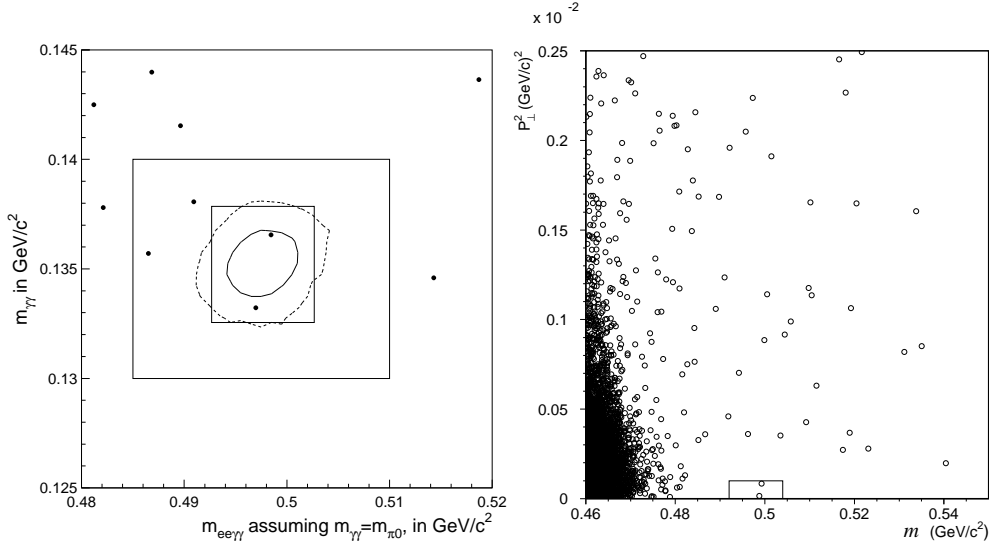


FIGURE 21. Signal planes showing candidates for $K_L \rightarrow \pi^0 e^+ e^-$ (left from Ref. [96]) and $K_L \rightarrow \pi^0 \mu^+ \mu^-$ (right from Ref. [97]).

power, it would require an experiment with a single event sensitivity of 0.77×10^{-14} , *i.e.* about 13,000 times that of the present one. Although not on the near horizon, sensitivities in this range have been discussed in connection with a proposed high-intensity proton driver at CERN [98]. The result is rather insensitive to the presence of the CP-conserving term, *but only as long as it is very well determined*, which, as discussed above, is not presently the case. Any uncertainty on the level to be subtracted dilutes the sensitivity and, for a given fractional uncertainty, the larger the CP-conserving component, the larger the impact on the sensitivity. For example, if $B^{CP-cons}(K_L \rightarrow \pi^0 e^+ e^-)$ is known to be 2×10^{-12} to 25% precision, it degrades the precision on $B^{direct}(K_L \rightarrow \pi^0 e^+ e^-)$ by only 10%. However, if $B^{CP-cons}(K_L \rightarrow \pi^0 e^+ e^-)$ is known to be 4.3×10^{-12} to 25%, this degrades the precision on $B^{direct}(K_L \rightarrow \pi^0 e^+ e^-)$ by 40%. The effects of the indirect CP-violating contribution are still more problematical because of the interference. Using Eqn. 11, Fig. 22 shows the measured CP-violating branching ratio vs the direct branching ratio for various plausible values of a_S . It is clear that for certain cases, such as $a_S = 1$, there is very little sensitivity to the direct branching ratio. On the other hand, since the CP-violating branching ratio can be much enhanced by the indirect part, for some values of a_S , the measurement gets considerably easier. Take the case of a negligible CP-conserving component and $a_S = -1$ and further assume that we have very good knowledge of $B(K_S \rightarrow \pi^0 e^+ e^-)$ and therefore of $|a_S|$. Then if $B^{direct}(K_L \rightarrow \pi^0 e^+ e^-) = 4.3 \times 10^{-12}$, $B^{CP-viol}(K_L \rightarrow \pi^0 e^+ e^-) = 27.9 \times 10^{-12}$. The expected result of the experiment described above would be 15,460 events over a background of 11,830, *i.e.* we'd have $B^{CP-viol}(K_L \rightarrow \pi^0 e^+ e^-) = (27.9 \pm 1.24) \times 10^{-12}$. This high value would immediately determine a negative sign for a_S and the result would then yield $\pm 15\%$ errors on $B^{direct}(K_L \rightarrow \pi^0 e^+ e^-)$, which more than meets our $\leq 20\%$ criterion. However, one will not know going in how well the experiment will work, since

the sign of a_S won't be known in advance.³

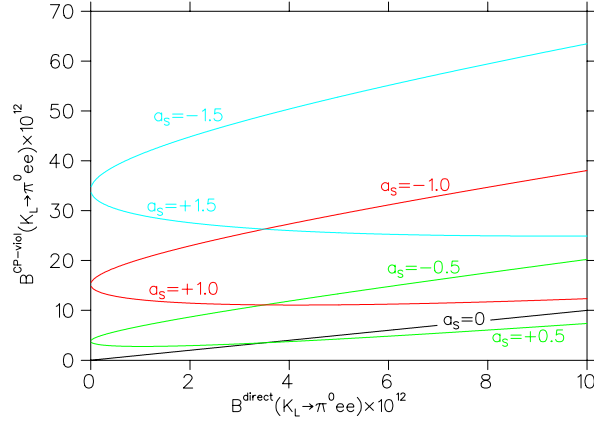


FIGURE 22. Relationship between $B^{CP-viol}(K_L \rightarrow \pi^0 e^+ e^-)$ and $B^{direct}(K_L \rightarrow \pi^0 e^+ e^-)$ for various values of a_S .

Thus, to make a useful measurement will require a 4 order of magnitude increase in signal statistics and both theoretical and experimental advances in the ancillary modes $K_L \rightarrow \pi^0 \gamma \gamma$ and $K_S \rightarrow \pi^0 e^+ e^-$, and still might not succeed. Various approaches for mitigating these problems have been suggested over the years including studies of the Dalitz Plot [99, 94], the $\ell^+ - \ell^-$ energy asymmetry [79] [94], the time development [100, 98, 94], or all three [101]. An innovative approach has recently been suggested [102] in which muon polarization in $K_L \rightarrow \pi^0 \mu^+ \mu^-$ as well as kinematic distributions are exploited. It's been known for many years that the μ^+ out-of-plane transverse polarization in this decay is sensitive to both the direct and indirect CP-violating amplitudes [78], and that one might be able to determine the sign of a_S through this. However, the individual effects of the direct and indirect amplitude are not easy to untangle using the transverse polarization alone. Ref. [102] assesses the potential of a number of polarization observables, and points out that the P-odd μ^+ longitudinal polarization is proportional to the direct CP-violating amplitude alone, even though it is not in itself a CP-violating quantity, whereas the branching ratio, the energy asymmetry and the out-of-plane polarization depend on both indirect and direct CP-violating amplitudes. As shown in Fig. 23, the polarizations involved turn out to be extremely large so that even with the polarization-diluting effect of the $K_L \rightarrow \gamma \mu^+ \mu^-$ background, enormous numbers of events may not be required to extract the direct amplitude. This method is reasonably clean theoretically and can determine the sign as well as the magnitude of that amplitude.

PION BETA DECAY

The sole current dedicated rare pion decay experiment is the PIBETA experiment at PSI. The primary objective of PIBETA is a precision measurement of the decay $\pi^+ \rightarrow \pi^0 e^+ \nu$.

³ It should also be kept in mind that Eqns. 11 and 12 are approximations.

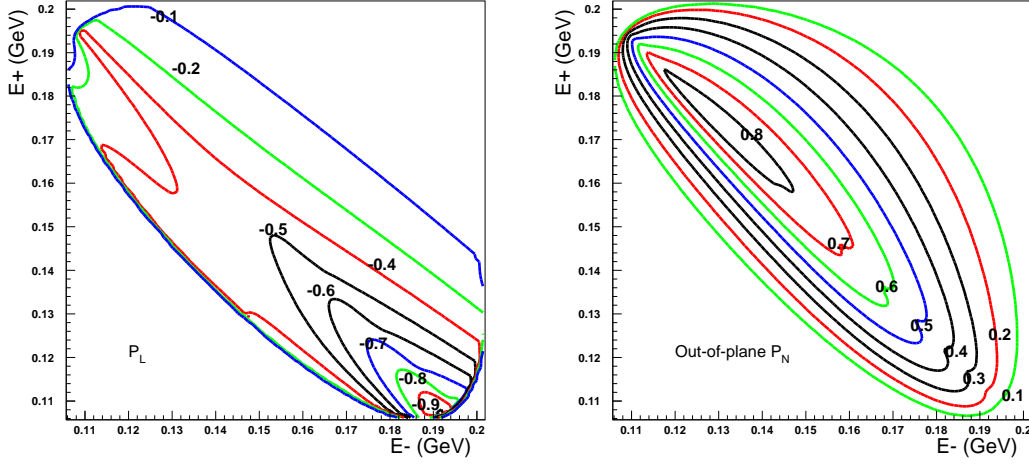


FIGURE 23. μ^+ polarizations in $K_L \rightarrow \pi^0 \mu^+ \mu^-$ from Ref [102] plotted against the muon cm energies. **Left:** longitudinal polarization. **Right:** out-of-plane polarization.

This is an example of a decay suppressed only by kinematics to the 10^{-8} level. The main interest in this decay is the determination of the CKM matrix element V_{ud} . There's a long-standing mystery in the experimental verification of the unitarity of the CKM matrix: the sum of the squares of the moduli of the first row of the CKM matrix does not quite add up to 1. Using the latest PDB values [18], $|V_{ud}| = 0.9734 \pm 0.0008$, $|V_{us}| = 0.2196 \pm 0.0026$, $|V_{ub}| = 0.0036 \pm 0.0007$ yields:

$$|V_{ud}|^2 + |V_{us}|^2 + |V_{ub}|^2 = 0.9957 \pm 0.0019 \quad (15)$$

i.e. a 2.2σ effect. The above value of $|V_{ud}|$ comes from measurements of nuclear beta decays and from neutron decay⁴. To explain the discrepancy of Eqn. 15, $|V_{ud}|$ would have to increase by 0.22%. This would result in a 0.45% increase in $B(\pi^+ \rightarrow \pi^0 e^+ \nu)$. There's $\leq 0.1\%$ theoretical uncertainty in the connection between this branching ratio and $|V_{ud}|$ [103], so it would be of considerable interest if a measurement on the $\leq 0.5\%$ level could be made.

Fig. 24-left is a layout of the PIBETA experiment. A ~ 1 MHz low energy π^+ beam is slowed from 113 MeV/c to 92 MeV/c in an active degrader and stopped in a 9-element segmented active target. Decays at rest are detected during a delayed $\sim 7\tau_{\pi^+}$ gate. Photons are detected in a 240-element CsI-pure array. One is basically looking for π^0 's in a small energy range following the decay of a π^+ . Detection of the very soft positron is not required, although it is often observed and used for systematic checks. The detector includes a tracking chamber surrounding the stopping target, that is used for other physics queries of the experiment, such as $\pi^+ \rightarrow e^+ \nu(\gamma)$ and $\mu^+ \rightarrow e^+ \nu_e \bar{\nu}_\mu \gamma$. Fig. 24-

⁴ Depending on how various data are weighted and what theoretical input is used, this discrepancy can be made as large as 4σ .

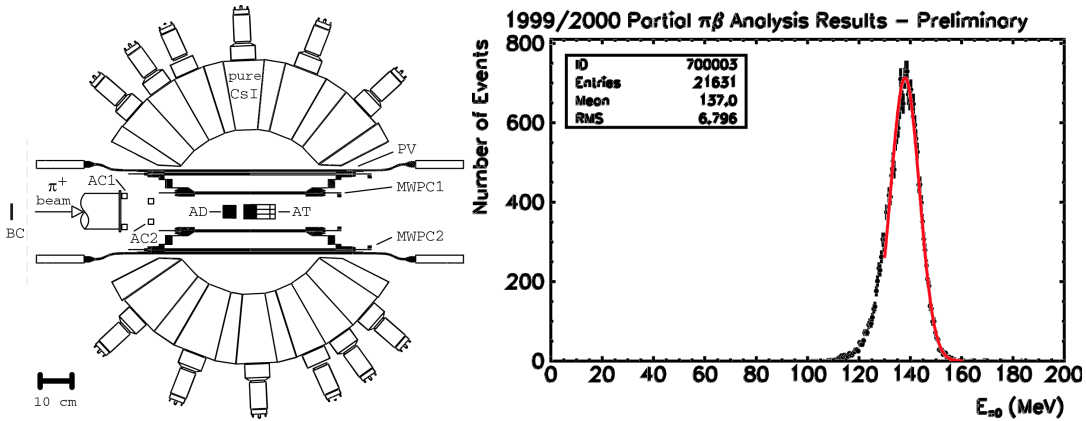


FIGURE 24. Left: Layout of the PIBETA $\pi^+ \rightarrow \pi^0 e^+ \nu$ experiment. Right: π^0 energy spectrum for $\pi^+ \rightarrow \pi^0 e^+ \nu$ candidates from PIBETA experiment.

right shows the π^0 energy spectrum from the 1999/2000 run. This is quite an impressive signal for a 10^{-8} -level decay. The branching ratio is normalized via a measurement of the decay $\pi^+ \rightarrow e^+ \nu$. There is a preliminary result $B(\pi^+ \rightarrow \pi^0 e^+ \nu) = (1.044 \pm 0.007_{stat} \pm 0.015_{sys}) \times 10^{-8}$ [104]. This is not yet sufficient to influence the unitarity problem, but it represents a factor 3 improvement on the previous measurement[105]. Further data is under analysis and an eventual statistical sensitivity of 0.33% is expected. An overall precision of $\leq 0.5\%$ is expected. To go significantly beyond this, one must reduce the systematic error due to the current precision on the normalizing branching ratio of $\pi^+ \rightarrow e^+ \nu$, which was last measured some ten years ago [106, 107, 108]. A separate experiment to improve the precision on this mode which would allow the full potential of PIBETA to be realized is in the planning stage. This decay is very interesting in its own right, in that it can severely constrain (or uncover) BSM physics by probing the limits of lepton universality [109].

$$K^+ \rightarrow \ell^+ \nu_\ell e^+ e^-$$

Recently AGS E865 has published data on the decays $K^+ \rightarrow \mu^+ \nu_\mu e^+ e^-$ and $K^+ \rightarrow e^+ \nu_e e^+ e^-$ [110]. These decays can proceed via inner bremsstrahlung (IB) off the ℓ^+ or the K^+ in $K^+ \rightarrow \ell^+ \nu_\ell$ or, more interestingly from the point of view of χ PT, via structure dependent (SD) radiation [111]. There can also be a contributions from the interference of these two amplitudes. At leading order in χ PT, the SD part is 0 so the decays go entirely by IB. At $O(p^4)$, the SD contribution is finite and can be characterized by constant form factors F_V, F_A, R , where the latter is related to the kaon charge radius. In principle there can also be a tensor amplitude characterized by a form factor F_T , although this is not allowed in the SM. However there have been hints of such an interaction in

other semileptonic weak decays [112, 113], so that it is of interest to allow for it in analyzing $K^+ \rightarrow \ell^+ \nu_\ell e^+ e^-$. At higher order in χ PT, the form factors can be functions of W^2 and q^2 , the effective mass squares of the $\ell^+ \nu_\ell$ system and the $e^+ e^-$ pair respectively. The IB term is helicity suppressed by a large factor in $K^+ \rightarrow e^+ \nu_e e^+ e^-$ but dominates $K^+ \rightarrow \mu^+ \nu_\mu e^+ e^-$. However one is sensitive to all three terms (IB, SD and interference) in the large q^2 region and so can hope to extract the signs of the form factors relative to that of the kaon decay constant, F_K .

Previous data on these modes have been limited to 4 events of $K^+ \rightarrow e^+ \nu_e e^+ e^-$ and 14 events of $K^+ \rightarrow \mu^+ \nu_\mu e^+ e^-$ [114]. E865 observed 410 $K^+ \rightarrow e^+ \nu_e e^+ e^-$ candidates including an estimated background of 40 events and 2679 $K^+ \rightarrow \mu^+ \nu_\mu e^+ e^-$ candidates including an estimated background of 514 events. Fig. 25 shows the missing mass distributions for the two samples. The corresponding measured branching ratios were $(2.48 \pm 0.14_{stat} \pm 0.14_{syst}) \times 10^{-8}$ ($m_{ee} > 150 \text{ MeV}$) and $(7.06 \pm 0.16_{stat} \pm 0.26_{syst}) \times 10^{-8}$ ($m_{ee} > 145 \text{ MeV}$) respectively [110].

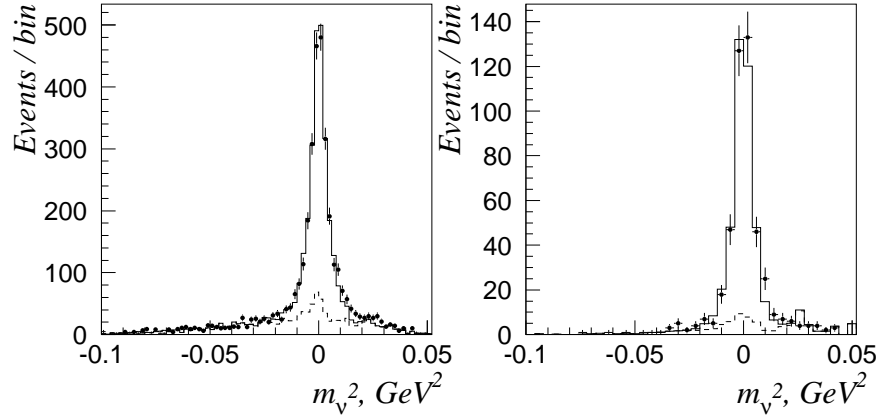


FIGURE 25. Missing mass distributions for **left:** $K^+ \rightarrow \mu^+ \nu_\mu e^+ e^-$ and **right:** $K^+ \rightarrow e^+ \nu_e e^+ e^-$. Dashed lines indicate background and solid lines simulated data.

Table 7 shows the results of a combined likelihood analysis by E865 in which $K^+ \rightarrow e^+ \nu_e e^+ e^-$ and $K^+ \rightarrow \mu^+ \nu_\mu e^+ e^-$ were fit simultaneously. This analysis assumed a resonance dominated form factor dependence on q^2 (the $\rho(770)$) and W^2 (the $K^*(892)$) for F_V and the $K_1(1270)$ for F_A and R . A fit assuming constant form factors had substantially lower likelihood. The “expected” values listed in the table are those of $O(p^4)$ χ PT supplemented by data from pion decay and in the case of R , from the measured value of the kaon charge radius [115]. The tensor form factor is consistent with 0, although the precision is not sufficient to rule out the effect postulated as an interpretation [116] of a result on $\pi^- \rightarrow e^- \bar{\nu}_e \gamma$ [112]. A new result on $\pi^+ \rightarrow e^+ \nu_e \gamma$ which will bear on this question is expected soon from the PIBETA experiment.

CONCLUSIONS

The success of lepton flavor violation experiments in reaching sensitivities corresponding to mass scales of well over 100 TeV has helped kill most models predicting acces-

TABLE 7. Results of a combined form factor analysis of $K^+ \rightarrow \ell^+ \nu_\ell e^+ e^-$ by E865 compared with expectations and with results from the pion sector. Units are 10^{-3} .

form factor	value \pm stat,sys,model	“expected” value	π^+ value
F_V	$112 \pm 15 \pm 10 \pm 3$	96	60 ± 28
F_A	$35 \pm 14 \pm 13 \pm 3$	41 ± 6	41 ± 6
R	$227 \pm 13 \pm 10 \pm 9$	230 ± 34	209 ± 30
F_T	$-4 \pm 7 \pm 7 \pm 0.4$	0	-5.6 ± 1.7

sible LFV in kaon decay. Thus new dedicated experiments in this area are unlikely in the near future. Since the most sensitive LFV limits in pion decay are parasitic to kaon experiments, similar remarks apply to them.

The existing precision measurement of $K_L \rightarrow \mu^+ \mu^-$ will be very useful if theorists can make enough progress on calculating the dispersive long-distance amplitude, perhaps helped by experimental progress in $K_L \rightarrow \gamma \ell^+ \ell^-$, $K_L \rightarrow 4$ leptons, etc. The exploitation of $K_L \rightarrow \mu^+ \mu^-$ would also be aided by higher precision measurements of some of the normalizing reactions, such as $K_L \rightarrow \gamma \gamma$.

$K^+ \rightarrow \pi^+ \nu \bar{\nu}$ will clearly be further exploited. Two coordinated initiatives are devoted to this: a 10^{-11} /event experiment (E949) just underway at the BNL AGS and a 10^{-12} /event experiment (CKM) recently approved for the FNAL Main Injector. The first dedicated experiment to seek $K_L \rightarrow \pi^0 \nu \bar{\nu}$ (E391a) is proceeding and an experiment (KOPIO) at the AGS with the goal of making a $\sim 10\%$ measurement of $Im(\lambda_t)$ is approved and in R&D.

Measurements of $K^+ \rightarrow \pi^+ \nu \bar{\nu}$ and $K_L \rightarrow \pi^0 \nu \bar{\nu}$ can determine an alternative unitarity triangle that will offer a critical comparison with results from the B system. If new physics is in play in the flavor sector, the two triangles will almost certainly disagree.

$K_L \rightarrow \pi^0 \ell^+ \ell^-$ will probably not be further pursued unless and until a BSM signal is seen in $K \rightarrow \pi \nu \bar{\nu}$.

ACKNOWLEDGMENTS

I thank D. Bryman, M. Diwan, S. Kettell, W. Marciano, D. Pocanic, R. Shrock, G. Valencia, and M. Zeller for useful discussions, access to results, and other materials. This work was supported by the U.S. Department of Energy under Contract No. DE-AC02-98CH10886.

REFERENCES

1. S.L. Glashow, J. Iliopoulos and L. Maiani, *Phys. Rev. D*, **2**, 1285 (1970).
2. Lee, B. W., and Shrock, R. E., *Phys. Rev.*, **D16**, 1444 (1977).
3. Cahn, R. N., and Harari, H., *Nucl. Phys.*, **B176**, 135 (1980), BOUNDS ON THE MASSES OF NEUTRAL GENERATION CHANGING GAUGE BOSONS.
4. Eichten, E., Hinchliffe, I., Lane, K. D., and Quigg, C., *Phys. Rev.*, **D34**, 1547 (1986).
5. Ambrose, D., et al., *Phys. Rev. Lett.*, **81**, 5734–5737 (1998).

6. Appel, R., et al., *Phys. Rev. Lett.*, **85**, 2450–2453 (2000).
7. Appel, R., et al., *Phys. Rev. Lett.*, **85**, 2877–2880 (2000).
8. Bellavance, A., *KTeV Search for $K_L \rightarrow \pi^0 \mu^\pm e^\mp$* (2002), talk given at DPF2002.
9. Hamm, J. C. (2002), FERMILAB-THESIS-2002-09.
10. Adler, S., et al., *Phys. Rev. Lett.*, **88**, 041803 (2002).
11. Adler, S. C., et al., *Phys. Rev.*, **D65**, 052009 (2002).
12. Baranov, V. A., et al., *Sov. J. Nucl. Phys.*, **54**, 790–791 (1991).
13. Belyaev, A., et al., *Eur. Phys. J.*, **C22**, 715–726 (2002).
14. Littenberg, L. S., *Phys. Rev.*, **D39**, 3322–3324 (1989).
15. Littenberg, L. (2000), talk given at 35th Rencontres de Moriond: Electroweak Interactions and Unified Theories.
16. Buchalla, G., and Buras, A. J., *Nucl. Phys.*, **B412**, 106–142 (1994).
17. Ambrose, D., et al., *Phys. Rev. Lett.*, **84**, 1389–1392 (2000).
18. Hagiwara, K., et al., *Phys. Rev.*, **D66**, 010001 (2002).
19. Aloisio, A., et al., *Phys. Lett.*, **B538**, 21–26 (2002).
20. Hocker, A., Lacker, H., Laplace, S., and Le Diberder, F., *Eur. Phys. J.*, **C21**, 225–259 (2001).
21. Hocker, A., Lacker, H., Laplace, S., and Le Diberder, F. (2001), CKM matrix Status and new developments.
22. Isidori, G., and Retico, A. (2002), $B/s, d \rightarrow 1+ 1-$ and $K(L) \rightarrow 1+ 1-$ in SUSY models with non-minimal sources of flavour mixing.
23. D’Ambrosio, G., and Gao, D.-N., *JHEP*, **07**, 068 (2002).
24. D’Ambrosio, G., Isidori, G., and Portoles, J., *Phys. Lett.*, **B423**, 385–394 (1998).
25. Gomez Dumm, D., and Pich, A., *Phys. Rev. Lett.*, **80**, 4633–4636 (1998).
26. Valencia, G., *Nucl. Phys.*, **B517**, 339–352 (1998).
27. Knecht, M., Peris, S., Perrottet, M., and de Rafael, E., *Phys. Rev. Lett.*, **83**, 5230–5233 (1999).
28. LaDue, J. (2002), talk given at DPF2002.
29. Alavi-Harati, A., et al., *Phys. Rev. Lett.*, **87**, 071801 (2001).
30. Alavi-Harati, A., et al., *Phys. Rev. Lett.*, **86**, 5425–5429 (2001).
31. Fanti, V., et al., *Phys. Lett.*, **B458**, 553–563 (1999).
32. Bergstrom, L., Masso, E., and Singer, P., *Phys. Lett.*, **B131**, 229 (1983).
33. Halkiadakis, E. (2001), FERMILAB-THESIS-2001-04.
34. Alavi-Harati, A., et al., *Phys. Rev. Lett.*, **83**, 922–925 (1999).
35. Zimmerman, E. D. (1999), doctoral thesis - University of Chicago.
36. Ambrose, D., et al., *Phys. Rev. Lett.*, **81**, 4309–4312 (1998).
37. Marciano, W. J., and Parsa, Z., *Phys. Rev.*, **D53**, 1–5 (1996).
38. Buchalla, G., and Buras, A. J., *Nucl. Phys.*, **B548**, 309–327 (1999).
39. Atiya, M. S., et al., *Nucl. Instrum. Meth.*, **A321**, 129–151 (1992).
40. Doornbos, J., et al., *Nucl. Instrum. Meth.*, **A444**, 546–556 (2000).
41. Chiang, I. H., et al., *IEEE Trans. Nucl. Sci.*, **42**, 394–400 (1995).
42. Adler, S. C., et al., *Phys. Rev. Lett.*, **79**, 2204–2207 (1997).
43. Adler, S. C., et al., *Phys. Rev. Lett.*, **84**, 3768–3770 (2000).
44. D’Ambrosio, G., and Isidori, G., *Phys. Lett.*, **B530**, 108–116 (2002).
45. Wilczek, F., *Phys. Rev. Lett.*, **49**, 1549–1552 (1982).
46. Buras, A. J. (2001), Flavor dynamics: CP violation and rare decays, Lectures given at the 1999 Lake Louise Winter Institute.
47. Buras, A. J., Gambino, P., Gorbahn, M., Jager, S., and Silvestrini, L., *Phys. Lett.*, **B500**, 161–167 (2001).
48. Buras, A. J., Colangelo, G., Isidori, G., Romanino, A., and Silvestrini, L., *Nucl. Phys.*, **B566**, 3–32 (2000).
49. Long, H. N., Trung, L. P., and Van, V. T., *J. Exp. Theor. Phys.*, **92**, 548–551 (2001).
50. Buchalla, G., Burdman, G., Hill, C. T., and Kominis, D., *Phys. Rev.*, **D53**, 5185–5200 (1996).
51. Xiao, Z.-j., Li, C.-s., and Chao, K.-t., *Eur. Phys. J.*, **C10**, 51–62 (1999).
52. Xiao, Z.-j., Lu, L.-x., Guo, H.-k., and Lu, G.-r., *Eur. J. Phys.*, **C7**, 487–499 (1999).
53. Chanowitz, M. S. (1999).
54. Hattori, T., Hasuike, T., and Wakaizumi, S., *Phys. Rev.*, **D60**, 113008 (1999).
55. Agashe, K., and Graesser, M., *Phys. Rev.*, **D54**, 4445–4452 (1996).

56. Bhattacharyya, G., and Raychaudhuri, A., *Phys. Rev.*, **D57**, 3837–3841 (1998).
57. Machet, B., *Mod. Phys. Lett.*, **A15**, 579–586 (2000).
58. Grossman, Y., *Nucl. Phys.*, **B426**, 355–384 (1994).
59. Gorbunov, D. S., and Rubakov, V. A., *Phys. Rev.*, **D64**, 054008 (2001).
60. Atiya, M. S., et al., *Phys. Rev.*, **D48**, 1–4 (1993).
61. Bassalleck, B., et al., *E949: An experiment to measure the branching ratio $B(K^+ \rightarrow \pi^+ \nu \bar{\nu})$* (1999).
62. Cooper, P. S., *Nucl. Phys. Proc. Suppl.*, **99N3**, 121–126 (2001).
63. Buchalla, G., and Isidori, G., *Phys. Lett.*, **B440**, 170–178 (1998).
64. Jarlskog, C., *Phys. Rev. Lett.*, **55**, 1039 (1985).
65. Grossman, Y., and Nir, Y., *Phys. Lett.*, **B398**, 163–168 (1997).
66. Alavi-Harati, A., et al., *Phys. Rev.*, **D61**, 072006 (2000).
67. Inagaki, T., *A plan for the experimental study on the $K_L \rightarrow \pi^0 \nu \bar{\nu}$ decay at KEK* (1996), talk given at 3rd International Workshop on Particle Physics Phenomenology, Taipei, Taiwan, 14-17 Nov 1996.
68. Bryman, D. A., and Littenberg, L., *Nucl. Phys. Proc. Suppl.*, **99B**, 61–69 (2001).
69. Glenn, J. W., et al. (1997), pub. in Vancouver 1997, Particle Accelerator, vol 1, 967-9.
70. Greenlee, H. B., *Phys. Rev.*, **D42**, 3724–3731 (1990).
71. Alavi-Harati, A., et al., *Phys. Rev.*, **D64**, 012003 (2001).
72. Alavi-Harati, A., et al., *Phys. Rev.*, **D62**, 112001 (2000).
73. D’Ambrosio, G., Ecker, G., Isidori, G., and Portoles, J., *JHEP*, **08**, 004 (1998).
74. Appel, R., et al., *Phys. Rev. Lett.*, **83**, 4482–4485 (1999).
75. Littenberg, L., and Valencia, G., *Ann. Rev. Nucl. Part. Sci.*, **43**, 729–792 (1993).
76. Batley, B., et al., A high sensitivity investigation of ks and neutral hyperon decays, Tech. Rep. SPSC/P253, CERN/SPSC2000-002 (1999).
77. Lai, A., et al., *Phys. Lett.*, **B514**, 253–262 (2001).
78. Ecker, G., Pich, A., and de Rafael, E., *Nucl. Phys.*, **B303**, 665 (1988).
79. Sehgal, L. M., *Phys. Rev.*, **D38**, 808 (1988).
80. Barr, G. D., et al., *Phys. Lett.*, **B242**, 523–530 (1990).
81. Papadimitriou, V., et al., *Phys. Rev.*, **D44**, 573–576 (1991).
82. Cohen, A. G., Ecker, G., and Pich, A., *Phys. Lett.*, **B304**, 347–352 (1993).
83. Capiello, L., D’Ambrosio, G., and Miragliuolo, M., *Phys. Lett.*, **B298**, 423–431 (1993).
84. Heiliger, P., and Sehgal, L. M., *Phys. Rev.*, **D47**, 4920–4938 (1993).
85. Kambor, J., and Holstein, B. R., *Phys. Rev.*, **D49**, 2346–2355 (1994).
86. D’Ambrosio, G., and Portoles, J., *Nucl. Phys.*, **B492**, 417–454 (1997).
87. D’Ambrosio, G., and Portoles, J., *Phys. Lett.*, **B386**, 403–412 (1996).
88. Kitching, P., et al., *Phys. Rev. Lett.*, **79**, 4079–4082 (1997).
89. Alavi-Harati, A., et al., *Phys. Rev. Lett.*, **83**, 917–921 (1999).
90. Lai, A., et al., *Phys. Lett.*, **B536**, 229–240 (2002).
91. Sehgal, L. M., *Phys. Rev.*, **D6**, 367 (1972).
92. Gabbiani, F., and Valencia, G., *Phys. Rev.*, **D64**, 094008 (2001).
93. Gabbiani, F., and Valencia, G. (2002).
94. Donoghue, J. F., and Gabbiani, F., *Phys. Rev.*, **D51**, 2187–2200 (1995).
95. Gabbiani, F. (2001), private communication.
96. Alavi-Harati, A., et al., *Phys. Rev. Lett.*, **86**, 397–401 (2001).
97. Alavi-Harati, A., et al., *Phys. Rev. Lett.*, **84**, 5279–5282 (2000).
98. Belyaev, A., et al. (2001), Kaon physics with a high-intensity proton driver.
99. Donoghue, J. F., Holstein, B. R., and Valencia, G., *Phys. Rev.*, **D35**, 2769 (1987).
100. Kohler, G. O., and Paschos, E. A., *Phys. Rev.*, **D52**, 175–180 (1995).
101. Littenberg, L. S., *CP violation in $K_L \rightarrow \pi^0 e^+ e^-$* (1988), in *Vancouver 1988, Proceedings, CP violation at KAON Factory* 19-28.
102. Diwan, M. V., Ma, H., and Trueman, T. L., *Phys. Rev.*, **D65**, 054020 (2002).
103. Marciano, W. J., and Sirlin, A., *Phys. Rev. Lett.*, **56**, 22 (1986).
104. Pocanic, D. (2002), talk given at the Workshop on the CKM Unitarity Triangle.
105. Mcfarlane, W. K., et al., *Phys. Rev. Lett.*, **51**, 249–252 (1983).
106. Britton, D. I., et al., *Phys. Rev. Lett.*, **68**, 3000–3003 (1992).
107. Britton, D. I., et al., *Phys. Rev.*, **D49**, 28–39 (1994).
108. Czappek, G., et al., *Phys. Rev. Lett.*, **70**, 17–20 (1993).

109. Bryman, D. A., *Comments Nucl. Part. Phys.*, **21**, 101–122 (1993).
110. Poblaguev, A. A., et al., *Phys. Rev. Lett.*, **89**, 061803 (2002).
111. Bijmens, J., Ecker, G., and Gasser, J., *Nucl. Phys.*, **B396**, 81–118 (1993).
112. Bolotov, V. N., et al., *Phys. Lett.*, **B243**, 308–312 (1990).
113. Akimenko, S. A., et al., *Phys. Lett.*, **B259**, 225–228 (1991).
114. Diamant-Berger, A. M., et al., *Phys. Lett.*, **B62**, 485–490 (1976).
115. Amendolia, S. R., et al., *Phys. Lett.*, **B178**, 435 (1986).
116. Poblaguev, A. A., *Phys. Lett.*, **B238**, 108–111 (1990).